ANTARCTIC ICEBERGS AS A GLOBAL FRESH WATER RESOURCE

PREPARED FOR THE NATIONAL SCIENCE FOUNDATION

J. L. HULT
N. C. OSTRANDER

R-1255-NSF
OCTOBER 1973

This report was sponsored by the National Science Foundation under Grant GI-34981. Reports of The Rand Corporation do not necessarily reflect the opinions or policies of the sponsors of Rand research.

Published by The Rand Corporation

ANTARCTIC ICEBERGS
AS A GLOBAL FRESH WATER RESOURCE

PREPARED FOR THE NATIONAL SCIENCE FOUNDATION

J. L. HULT
N. C. OSTRANDER

R-1255-NSF
OCTOBER

Rand
SANTA MONICA, CA. 90406

PREFACE

This report is intended to provide background knowledge for potential users and suppliers of Antarctic icebergs, and for governments or agencies concerned with the development, regulation, or control of the use of these valuable ice resources.

The research reported herein has been sponsored principally by the Directorate of Research Applications, Office of Exploratory Research and Problem Assessment of the National Science Foundation, under its programs for Research Applied to National Needs (RANN).

The major areas discussed in the report include:

- An orientation about preliminary concepts for using Antarctic iceberg resources.
- Some preliminary feasibility estimates.
- Some of the principal problems and promises that seem to warrant further investigation.

The results of various phases of the investigation will be published in later reports as work progresses on expanding the concepts and refining the technological feasibility. Among those areas that will be developed further are:

- A more detailed analysis of the applicability of Earth Resources Technology Satellites (ERTS) in the harvesting of Antarctic iceberg resources.
- A study and comparison of the more promising techniques for converting icebergs to fresh water with deference to environmental considerations.
- The description of experiments using real icebergs to test alternative operational system designs.
- The assessment of societal and environmental impacts.

The authors wish to acknowledge the assistance, comments, and sources of information provided by H. Kenneth Gayer of the National Science Foundation; the review and comments of Rand colleagues James C. DeHaven and Charles L. Freeman; and the painstaking editing of Margaret Milstead. Many others also contributed by private communications as well as through cited references. The authors accept the responsibility for any errors of fact or interpretation.

SUMMARY

As population soars and standards of living increase, the fresh water deficiencies in certain areas of the world are rapidly becoming acute. Those areas that are particularly concerned include the Pacific Southwest United States, and parts of Mexico, Chile, Australia, the Middle East, and North Africa. In some of these arid regions, water may be available by transferring it from river basins with abundant water or by desalting seawater. However, the costs of transferring or desalting, which may be $100 or more per acre-ft,[1] tend to put severe limits on such use.

For the thirsty areas of the world, the possibility of using Antarctic icebergs as a fresh water resource might become a very attractive prospect. The crucial problem is to devise a technology that can deliver melted iceberg water at much less cost than either desalting or interbasin transfers, while at the same time ensuring acceptable environmental impact of such operations.

The idea of using Antarctic icebergs has been considered and even tried a number of times during the past century. Theoretically, icebergs could be floated to any point accessible by a deep water route (at least 200 m of water depth).

The abundance of icebergs has long been recognized (annual yield of about 1000 million acre-ft or 1,000,000 million cubic meters). If a way can be found to move the icebergs and control their melting so as to deliver, say, 10 percent of the *annual* yield economically, this operation could potentially satisfy the water demands of an urban population of 500 million (with a usage of 200 m^3 per person). The potential direct economic impact of fully exploiting 10 percent of the annual yield is estimated to be as much as $10 billion annually.

Past exploration of the Antarctic has indicated that a major portion of the sea ice that forms and builds up during the dark winter months thaws out during the daylight season. By March of each year most of the tabular icebergs naturally formed from the ice-shelf discharges are accessible for acquisition and export operations. Although the *sea* ice is generally less than 2 m thick (compared with a few hundred meters for most tabular, fresh water icebergs), the area of sea ice formed and thawed each year is thousands of times the total area of icebergs and about ten times the mass. Thus sea ice is a major factor to contend with in the acquisition of icebergs. Its moderating influence on the climate (together with that of the continental icecap) is so dominating over that of the icebergs that little climatic effect would be expected, even with the complete removal of the total annual iceberg yield. It

[1] An acre-ft of water is a quantity sufficient to cover one acre with water a foot deep.

should be possible to process icebergs for high quality fresh water and thermal pollution abatement without adverse effects on the global or Antarctic climate.

The NASA Earth Resources Technology Satellite (ERTS) Program is providing valuable pictures that show how the sea ice recedes during the daylight season, and that give the locations, movements, and dimensional characteristics of icebergs of interest. Early interpretation confirms the general abundance of icebergs and sea ice behavior demonstrated in previous exploration data. Detailed statistics about iceberg dimensional characteristics will become available with more complete pictures, and when appropriate sampling of dimensional measurements have been made and analyzed. It will then be possible to estimate how easily a certain fraction of the icebergs can be collected into various "train" configurations, and project the corresponding costs associated with their delivery to terminal locations.

In order to get a better understanding of the feasibility of moving icebergs and controlling their melting, a model of the transport operations from the Ross Sea to Southern California was made. The available environmental data on currents, winds, and temperatures were included in the model. Although these data are very crude and limited, they are adequate to test the preliminary feasibility. The model shows that the transport effort required need not be very sensitive to the winds, can benefit from the currents but is not dependent on them for feasible operations, is not too sensitive to the route selected, and will require insulation of the icebergs for acceptable survival en route to the Northern Hemisphere. The Coriolis forces,[2] which are proportional to the momentum (mass $\times$ velocity) and the sine of the latitude, provide the principal resistance to the transport operations. These forces are applied at right angles to the velocity and require a large fraction of the transport effort to counteract their effects, particularly at more southerly latitudes.

The cost of delivering the icebergs will be determined by the design of the transport operations and the configuration of the iceberg "trains." Narrow trains (300 to 600 m wide) are desirable because they are estimated to reduce the net Coriolis effects on the icebergs. Also, when these trains are propelled at an angle with respect to the resultant velocity, they can more effectively obtain "lift" to counteract Coriolis forces. An asymptotic minimum transport effort per unit of iceberg is approached for iceberg "trains" longer than about 20 km. Greater lengths increase the mass, transport resistance, and insulation costs proportionately. The costs of insulation can be estimated without specifying many of the details of operational techniques for applying the insulation, which need to be tested by experience. Essentially, the iceberg surfaces exposed to ablation from the flowing seawater can be wrapped by unrolling plastic film that is designed to trap pockets of melt water to form a quilting of still water between the iceberg and the flowing seawater. Quilt-water thicknesses of 3 cm will limit the iceberg melting to less than 10 percent per year.

The operational cost of delivering a large iceberg train (1.22×10^{13} kg) to California on a one-year cycle is estimated to be about \$8 per 1000 m^3 (\$10 per acre-ft). It is also estimated that designing operations for more nearly optimum speed or better train configurations will not significantly reduce these rates. On the other hand, these delivery costs should approximately hold for a variety of operations that would depart significantly from the asymptotic one that was costed.

[2] Coriolis forces tend to deflect an object moving in the Northern Hemisphere to the right and one moving in the Southern Hemisphere to the left.

The Summary Figure shows a possible operational configuration with electrically driven propellers distributed along, and harnessed to, the train convoy. Also shown is a possible test configuration using more conventional tugs to pull a small three-piece iceberg train.

Before designing and developing an operational system, and for refining cost estimates, a test program with icebergs would be desirable to: determine the nature of the submerged surfaces of tabular icebergs; test techniques for insulating and harnessing icebergs; measure the transport environment and performance; determine how well the Coriolis forces can be controlled; and test the performance of modeling to simulate operational control and performance.

The conversion of the icebergs for fresh water and heat sink is explored in a very preliminary way in order to uncover promising concepts and to estimate cost limits based on general physical principles. This exploration indicates that iceberg conversion to fresh water at sea level should be achievable in a variety of ways for about \$8 per 1000 m^3. A preliminary engineering study and comparison of the more promising conversion techniques is needed to develop better cost estimates and the basis for the design of test systems for evaluating alternative approaches for operational systems.

The total costs of Antarctic iceberg transport, conversion to water, and delivery to wholesale distribution terminals in coastal areas appear to be of the order of \$30 per acre-ft. This would be less costly and would require less energy expenditure than interbasin water transfers of a few hundred miles or desalting or costly water reclamation operations. Furthermore, nuclear energy could be used, thus eliminating competition for fossil fuel resources. Fresh water from icebergs should therefore become an attractive alternative for areas close to deep seawater access routes.

Before any large-scale operational use of Antarctic icebergs is implemented, there should be a comprehensive assessment of the potential societal and environmental impacts. A preliminary exploration of a variety of such factors reveals no obvious insurmountable obstacle. The factors to be investigated include: the international acceptability of exploiting Antarctic icebergs; the en route environmental constraints; the acceptability of terminal operations; the demand for iceberg water and the integration of its delivery system with other established systems for furnishing fresh water; icebergs as reservoirs and recreation areas; and the risk involved in implementing iceberg water resource systems. The more avenues that are explored, the more promising the concepts seem to become. However, a more refined assessment can be made when the potential operations become better defined, and when specific terminal applications can be examined in detail.

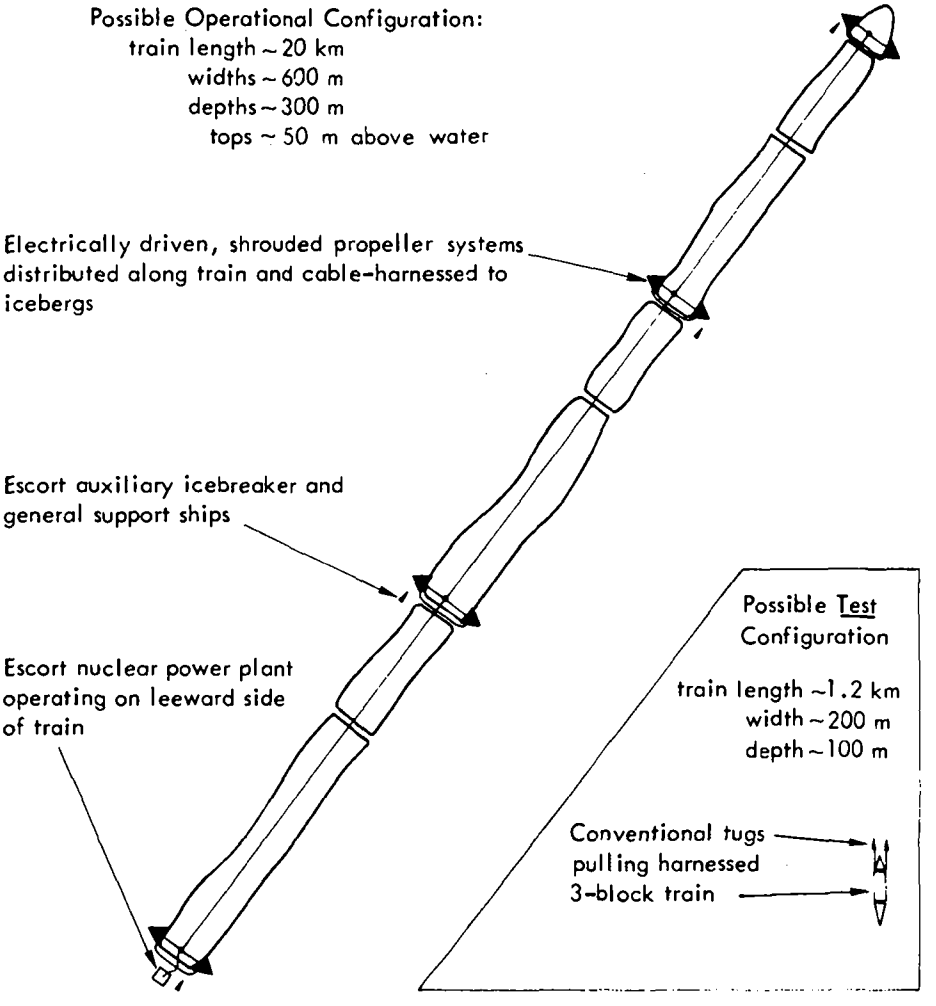

Summary Fig.—Conceptual illustrations

CONTENTS

Appendices have been included to provide technical background details that are not readily obtained from published references. In addition to the references, a selected bibliography provides useful background information.

II. POTENTIAL FRESH WATER DEMANDS AND RESOURCES

DEMAND FOR FRESH WATER

There are increasing expressions of concern that there be adequate potable water for the sustenance and future development of society [6-17]. The United States is well-endowed with water from the average annual precipitation, about 3/4 m, which is approximately the world average over land. Most of the precipitation is returned to the atmosphere by evapotranspiration processes; only about one-fourth is left for withdrawal and controlled use. In the conterminous United States, this water averages about 1.2×10^{12} gallons per day (about 10^9 acre-ft[1] per year, or 1.23 T•m^3 per year[2] [9]. This amount is estimated to be adequate for the total U.S. demand during this century if the water is used efficiently. However, problems will increasingly arise over water quality and regional supply. In particular, water deficiencies in the Pacific Southwest (including the basins drained by the lower Colorado River) have led to large projects like the California State Water Project and the Central Arizona Project for importing water overland in amounts of millions of k•m^3 per year at the total costs of \$50 to \$100 per k•m^3. These projects do not, however, adequately satisfy the basic water deficiencies of the lower Colorado River basin. The metropolitan areas in these regions use an average of 200 to 300 m^3 per capita per year. Furthermore, the irrigation demands in these arid regions, which represent the largest consumptive use of water, call for nearly 2 m^3 per year per m^2 of irrigated area.

As a result of a treaty with Mexico, the United States is obligated to see that an average of 1.5 million acre-ft of Colorado River water flow across the border annually. Since laws and treaties have overly committed the likely yield of Colorado

[1] An acre-ft of water is a quantity sufficient to cover one acre with water a foot deep.

[2] The International System (SI) of metric unit notation will be used frequently in this report, although some more traditional American forms of unit notation will also be used.

$$1 \text{ acre-ft} \simeq 1234 \text{ m}^3 \simeq 1.23 \text{ k•m}^3$$
$$10^6 \text{ acre-ft} \simeq 1.23 \text{ G•m}^3$$
$$10^9 \text{ acre-ft} \simeq 1.23 \text{ T•m}^3 = 1.23 \times 10^{12} \text{ m}^3$$

Care should be taken to distinguish between a cubic kilometer (km^3) and the authors' special notation of a thousand cubic meters (k•m^3).

$$1 \text{ km}^3 = 10^9 \text{ m}^3 = 10^6 \text{ k•m}^3$$

River water, the federal government has undertaken the obligation of augmenting the Colorado River in order to satisfy the Mexican treaty.

Two methods for augmenting the Colorado have been considered. The first method calls for interbasin transfers, which will probably cost up to \$100 per k•m³. The second method involves large seaside desalting plants that would convert seawater into fresh water at costs hopefully around \$100 per k•m³. These water costs are easily justified for many industrial, commercial, and domestic urban uses; however, the largest demand for water in arid regions is for agriculture.

Studies indicate that the primary direct benefits of using water for large-volume agricultural purposes in the belt from Southern California to Texas could be valued from a few dollars to about \$35 per k•m³. Adding secondary benefits, this range could be increased from \$24 to more than \$40 per k•m³ [18]. These studies have also explored the marginal costs for the alternative methods of water supply without evaluating the water quality. In many areas, the poor quality of even current water supplies is inhibiting agricultural productivity. Since either interbasin transfers of water or desalting processes would cost about \$100 or more per k•m³, any alternative method for delivering good quality water at substantially lower cost to the Pacific Southwest should be in strong demand. It appears that iceberg water could be imported to this area to satisfy demands for millions of acre-ft of water for municipal and industrial uses at \$50 per k•m³ and for many millions of acre-ft of water for agricultural uses at \$30 per k•m³.

Similar urban, industrial, and agricultural demands for water should develop before the turn of the century in many arid regions of the world (Fig. 1). Portions of Israel and adjacent areas, Mexico, Chile [19], and Australia [16] should manifest such demands in the near future. Other latent water demands in Africa and Asia may take longer to develop into large volumes. Once the practicability of using iceberg-water resources has been demonstrated, a significant demand for this water may quickly develop in accessible, populated coastal areas of the world that are not

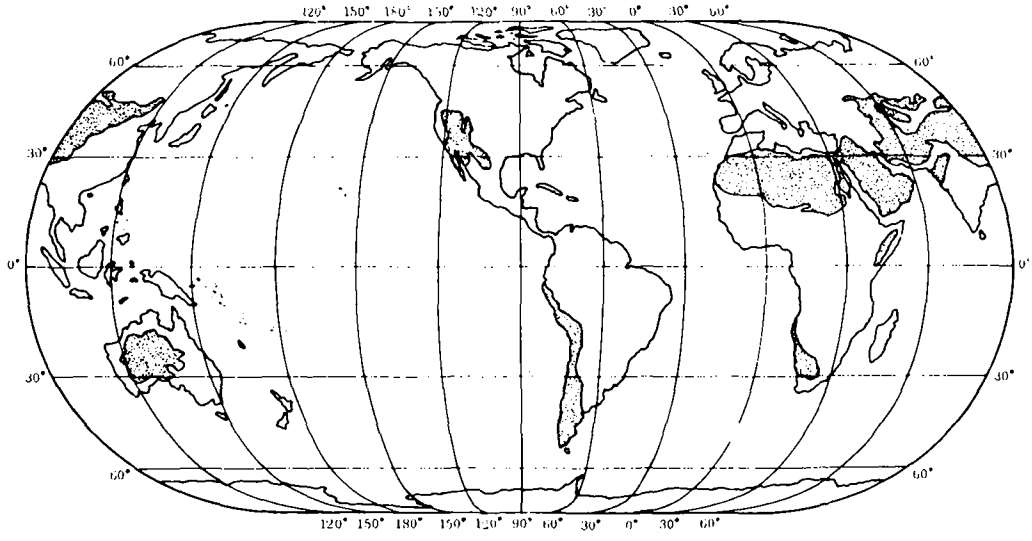

Fig. 1—Arid regions of the world (shaded)

considered arid—for example, Japan. Taking all these potential demands into consideration, it appears that Antarctic icebergs will become an attractive source of high-quality, economical fresh water for the United States and for much of the rest of the world as well.

The water-deficient Pacific Southwest is becoming highly industrialized and, due to large power consumption, is increasingly concerned with thermal pollution. Homes, automobiles, and other personal energy consumption also contribute significantly to the thermal pollution. It has been estimated that the total heat load per capita injected into the environment in the United States averages about 10 kW (about 2 kW in the home, 2 kW for transportation, 3.5 kW for industry, and 2.5 kW for commercial and other purposes) [20]. If this *total* heat load per capita were used to melt icebergs, the resulting melt water could supply about 20 percent of the per capita water used by current standards. In the Southern California area, the total waste heat from electrical power generation could currently be absorbed with less than a million acre-ft of icebergs per year. Thus icebergs as heat sinks may have significant (though as yet undetermined) value in the abatement of thermal pollution.

POTENTIAL FRESH WATER RESOURCES

The world's total water resources are estimated to be 97 percent seawater and only 3 percent fresh water [21]. Three-fourths of the fresh water is held in the form of ice, most of it (about 90 percent) in the Antarctic. In the Antarctic water cycle (precipitation-evaporation-precipitation), water is locked up in glacial form for thousands of years before it is melted and returned to the sea. This long storage period in the form of flowing ice explains why such a large portion of the world's total fresh water inventory at any time is contained in ice.

The Antarctic continent, including its ice shelves[3], has an area of approximately 13.975 $T \cdot m^2$ (approximately 5.4 million sq mi) [22]. Although estimates from sampling annual accumulation vary considerably, the values taken from the Antarctic Atlas [22] (illustrated in Fig. 2) indicate an average annual ice accumulation equivalent to about 17 cm of water or a total of about 2.4×10^{15} kg per year. The accumulation is greatest on the northern edges of the continent near sea level, with annual values ranging for the most part between 20 and 60 cm of water equivalent. In the high interior regions, this accumulation diminishes to less than 5 cm per year. As new ice accumulates and packs down previous snow accumulations, the specific gravity of ice farther than about 60 m down (a few hundred years of accumulation) asymptotically approaches the specific gravity of solid ice (0.92). The total mass of accumulated non-seawater Antarctic ice is estimated to be about 2.4×10^{19} kg, or the equivalent of 10,000 years of annual accumulation [23]. It has of course taken much longer than 10,000 years to accumulate, because the annual accumulation has for thousands of years been nearly balanced by the annual losses to the sea.

Glacial ice is plastic and gradually flows downhill toward the sea. Most of the

[3] Ice *shelves* are the layers of ice that extend off the land and float on water. The ice *sheet* is the total ice covering over Antarctica. An ice *stream* may be a glacier or any other conduit where ice flow or movement is concentrated.

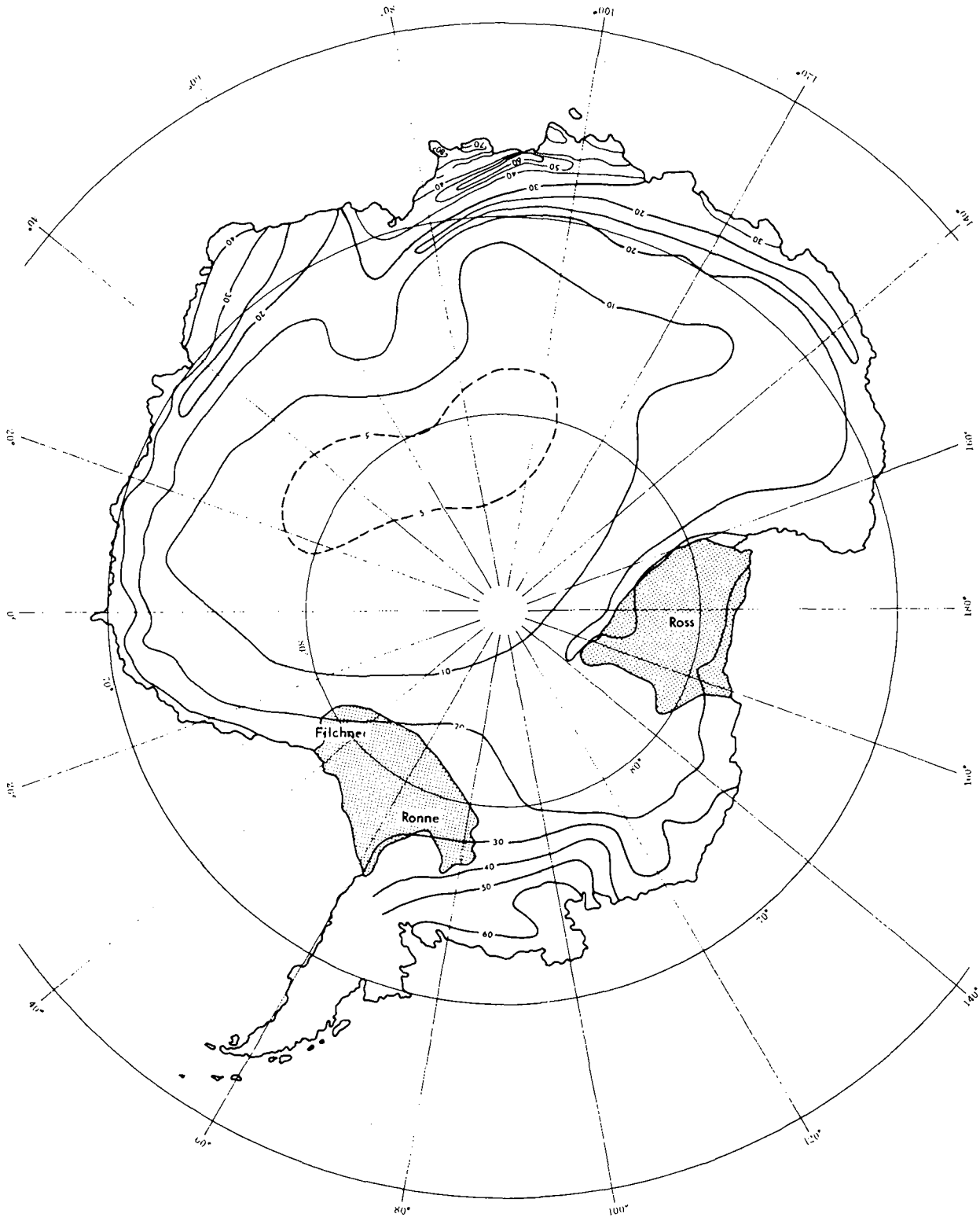

Fig. 2—Accumulation contours in Antarctica
(in centimers of water equivalent)

colder top portions tend to move as rigid blocks, both overland in the ice sheet and overwater in ice shelves; the ice flow has boundary layers so that there is very little shear flow outside of the immediate vicinity of obstructions or boundary resistance. The tendency for an ice shelf to approach uniform thickness (behind the local variations due to differences in bottom melting near the ice front) can produce rotating or swinging plate flow in shelves with unevenly distributed inputs. All the ice stream inputs to an ice shelf accelerate and contribute to its plate-like flow even to the point of drawing the "plate" thinner in areas of smaller input. The grounded ice sheet is estimated to move an average of about 20 m per year, whereas the flow rate for the ice shelves and most ice streams is generally more than 300 m per year [24]. Thus, because of this faster movement, ice streams and shelves account for most of the ice loss to the sea.

The Ross Ice Shelf is the largest in area and most accessible, and constitutes about one-third of the Antarctic ice shelf. The less accessible Ronne-Filchner Ice Shelves together are nearly as large. All the remaining small ice shelves in total are approximately equivalent to the Ross Ice Shelf. We will, therefore, describe the typical evolution of icebergs and ice loss as they occur at the Ross Ice Shelf.

The flow of ice in the Ross Shelf (see Appendix A) tends to move in rigid blocks, with most of the resistance or flow-rate changes appearing near edges or grounding points. At the sea-front edge of the ice shelf, the average discharge velocity of ice is about 700 m per year. Most parts of the shelf spend more than 1000 years from launch until discharge into the sea. During this period nearly 200 m of ice accumulate on top and most of the originally land-launched shelf melts off the bottom. Thus the icebergs that calve or break off of the seaward edge have largely been formed on the ice shelf. Much of the discharge from the Ross catchment is melt from under the shelf. The melting rate is the greatest on the seaward edge, and, in particular, the tongue extending north of 78° latitude in the vicinity of Ross Island appears to experience bottom melting rates between 1 and 10 m per year from the strong undercutting currents that sweep in and under from the northeast and exit out of McMurdo Sound. However, the melting rates seem to exceed the accumulation rates over most of the shelf which is consistent with a net mass balance for all of the Ross catchment. The inner bottom-melting rates could be explained by the convective ventilation induced by the large turbulent flow associated with the tidal breathing under the shelf (see Appendix A).

When the ice shelves or calved icebergs project out to sea so that their bottoms are exposed to the uninhibited ocean currents, they should experience melting rates of tens of meters per year and have average lifetimes of less than 10 years.

A similar loss process can be expected for the Ronne-Filchner catchments and those of all the other ice shelves. However, in the case of the shallow shelves, bottom melting may contribute a smaller fraction of the total loss. Thus, as is indicated in Appendix A, the Antarctic could be nearly in mass balance with about half of the accumulation lost in icebergs and the other half in melt from under the ice shelves. The net annual yield of icebergs could then be about 1.2×10^{15} kg, and the total iceberg accumulation in the Antarctic oceans has been estimated to be about six times this quantity [25], which would correspond to an average iceberg life in the southern oceans of about 6 years.

A limited survey of the icebergs in East Antarctica [26] has indicated that icebergs have a mean length of greater than 1 km and a mean height above water

of about 50 m. However, large tabular icebergs with top surface areas of thousands of square kilometers have been observed, and many icebergs have been found with horizontal dimensions of 0.3 to 10 km. If a horizontal dimension is comparable to the vertical thickness, the iceberg is not very stable and may roll over and deteriorate rapidly. Thus, the quantity of icebergs with horizontal dimensions less than about 0.3 km falls off rapidly. However, there should be no problem in finding icebergs of widths up to 1 km and lengths up to several kilometers. A survey of the quantity and distribution of various iceberg sizes in the Antarctic is being made with the Earth Resources Technology Satellites. This should confirm the abundance of the desired sizes and shapes of icebergs in the Antarctic, as well as establish the suitability of satellites as an aid in the efficient harvesting of icebergs.

The total quantity of precipitation (i.e., non-seawater) ice that is melted each year in the Antarctic is approximately equal to the total accumulation—2.4×10^{15} kg. However, the sea ice that is frozen and melted each year in the Southern ocean is about 10 times this quantity and thousands of times the area [25]. So, sea ice in the Antarctic is a much more important moderator of the annual fluctuations in the earth's surface temperature than precipitation ice is. Sea ice forms and melts near the surface of the ocean as a function of season and surface conditions. Iceberg bottoms, on the other hand, are deeply submerged and may experience more continuous year-round ablation from the deeper ocean currents.

Sea ice commences to form in March-April in the Antarctic and locks up an increasing area, including icebergs, until October. The daylight season thaws the shallow sea ice (average 1-2 m thick), and most of the icebergs of interest become unlocked by January-March for easiest collection into iceberg trains. The most efficient method for harvesting Antarctic icebergs is therefore likely to be based on a 1- or 2-year transporting cycle, with the acquisition and iceberg-train formation taking place during the daylight season.

Antarctic icebergs have been found to be remarkably free of impurities (a few parts per million) because they are formed from precipitation in a relatively pollution-free atmosphere, and the large tabular icebergs are practically all carried to sea in the ice shelves where most of the bottom-rafted debris is melted and dropped off [27]. Even if the processed iceberg melt water were contaminated with 1 percent of seawater, it would still have a lower salt content than most land-derived water supplies. Colorado River water, for example, has a salt content (more than 700 parts per million) equivalent to 2 percent or more of ocean water.

POTENTIAL ECONOMIC IMPACT

The estimated, total, continuous yield of icebergs from the Antarctic is 1.2×10^{15} kg per year, which could be harvested beneficially and without depletion or environmental damage in the Antarctic. The total yield is the equivalent of 1.2×10^{12} m^3 of high quality fresh water, which would be adequate to satisfy the needs of an urban population of 4 to 6 billion people at 200 to 300 m^3 of water per capita per year. This is the current standard rate of consumption in the urban areas of the U.S. Pacific Southwest. This total annual water resource might alternatively be used to irrigate 0.6 to 1.0×10^{12} m^2 (~150 to 250 million acres) or more of agriculture.

If the total potential iceberg resources were exploited (1.2×10^{15} kg per year), the transporting of the icebergs would ultimately involve an annual business of about $10 billion per year (at about $10 per k•m³ or acre-ft). The total cost of delivery for wholesale distribution of high quality fresh water would be about $30 billion to $50 billion per year ($30 to $50 per k•m³ or acre-ft). The savings over desalting or long-distance interbasin transfer could ultimately amount to $50 billion to $70 billion per year ($50 to $70 per k•m³ or acre-ft). The complete efficient harvesting and full exploitation of the Antarctic iceberg resources should not be expected for many years. An estimate of the maximum development and use that might be anticipated by the end of this century is illustrated as follows:

	Millions of k•m³ or acre-ft
United States and Mexico	30
Australia	10
South America	10
Middle East	10
Africa	10
Japan and West Pacific Islands	10
Maximum estimated total by year 2000	80

This would amount to less than 10 percent of the potential harvest, but it would have a direct economic impact of $2 billion to $5 billion per year.

There are a few special impacts that may be worth mentioning in this preliminary assessment. The energy costs are a significant portion of the total costs involved in any acquisition of good quality water. Energy consumption should be less per unit of water supplied from Antarctic icebergs than from most interbasin transfers or desalting operations. Thus the use of iceberg water may permit important savings in energy consumption. Furthermore, there are attractive opportunities and advantages for using atomic energy rather than fossil fuels in the importation of Antarctic icebergs. Also, advanced technology plus large investments are advantageous for exploiting the enormous fallow Antarctic-iceberg resources. This should be an attractive opportunity for the United States to employ its skill and technology in harvesting and delivering Antarctic ice for the benefit of its foreign exchange.

III. TECHNOLOGICAL FEASIBILITY

ACQUISITION OF POLAR ICE

The previous discussions have indicated little doubt of the general adequacy of suitable icebergs to satisfy the projected demands. However, it has not yet been made clear where, when, how, and at what cost the desired icebergs can be acquired to accommodate a specific demand. Transporting icebergs through the Pacific to the west coasts of the Americas, and even as far east as the coast of Japan, would probably call for acquiring icebergs in the region west of the Antarctic peninsula from west longitudes of about 75° through the Ross Sea. This sector, which includes the Ross Ice Shelf, should prove to be the best region for obtaining icebergs for the Pacific areas. It may be better to transport icebergs for Africa, the Middle East, and Australia (via the Atlantic and Indian Oceans) from East Antarctica.

If a single small iceberg is needed, the acquisition could probably be made almost any time of the year at south latitudes between 60° and 65° for transport through the Pacific, and between 55° and 60° for transport through the Atlantic and Indian Oceans. However, to make the collection of large quantities of icebergs into trains an economical operation, it will probably be necessary to make the acquisitions farther south where the density of icebergs increases. Such operations at the more southerly latitudes are likely to be most successful during November to March when more daylight is available and sea ice is receding and thus less inhibiting to the acquisition operations.

For more efficient acquisition and formation of iceberg trains, satellites might search for the most convenient locations of clusters of appropriate iceberg sizes and shapes. The photographic resolution of the Earth Resources Technology Satellites (ERTS) is well suited to the task, but the best sensor is likely to be a long wavelength (8 to 14 micrometers), which should not be as dependent on solar illumination. The capability of ERTS-1 for accomplishing this function with shorter (less than 1.1 μm) wavelengths is being explored. Early indications are that cloud cover may be the most serious limitation, but that satellites should still be able to accomplish the job satisfactorily.

Once the appropriate clusters of suitable icebergs have been located, the selection and preparation for train formation can be initiated. For trains smaller than about 10^6 k•m^3, the shape and positioning of individual icebergs within the train are important because the resistance from form drag is relatively large. With larger

trains, skin friction and Coriolis forces[1] tend to dominate the resistance, and the train design will emphasize "lift" to counteract Coriolis effects. These factors will be discussed in more detail in the following subsection.

In selecting iceberg blocks for a train, it will be necessary to check for acceptable dimensions and surfaces and to prepare them for the application of insulation and harnesses. Also the blocks in a train formation should be arranged to minimize the perturbations in the boundary-layer flow along the train. The preparations that might be required are more easily visualized by illustrating a method for insulating the icebergs. However, we do not claim that this method is a superior one with respect to cost or effectiveness. Easily manageable rolls of plastic film about 3 m wide would be unrolled and wrapped around and under the iceberg along its width. In this way, each lap around the iceberg would not require more than one roll of film. Only the sides and bottom would need to be covered for insulation. The topside could be used to cinch the loop and sink the cinch edges of the film into the ice to anchor it against downstream skin friction pull.

The rolls of film might consist of two layers of thin film with the layer next to the ice interlaced with a waffle network of tension cords (at, say, 0.2 m spacing) and with the two layers of film laminated together on the edges with the major cinching cords. As the tension cords sink into the ice they would trap melt water in the waffle quilt pattern to form pockets (≈0.2 m on a side) of trapped water under the stretched film. The heat transfer from the outside film to the iceberg would then be primarily by conduction through the entrapped water layers, which would serve as a very effective insulator from the outside boundary-layer stream. The successive rolls of film and insulation could be applied from the back toward the front of the iceberg so as to overlap the layers in a manner analogous to the scales on a fish. The amount of overlap could be arranged to meet the insulation and skin-friction pull requirements at each location along the length of the train. There is no need to make the wrapping watertight. The objective is to reduce the convective flow to the point that conduction becomes the controlling mode of heat transfer.

The underwater preparation of the icebergs would involve passing a weighted cable under the iceberg between two tugs and then trimming undesirable edges or configurations that could jeopardize insulation operations. The cable could then be tied in an endless loop around the iceberg and, with appropriate topside winches, the cable could pull a tracking, ice-grooving, and film-unrolling mechanism around the bottom side of the iceberg. The laying of each lap of film insulation would probably require about 1/3 hour (rolls spaced 600 m apart on the endless winch loop pulled at 0.5 m/sec) so that each kilometer of iceberg length would require 100 to 300 hours for wrapping the insulation, depending on the overlap that is used. Thus it is possible that the iceberg blocks to which the propellers are attached could be insulated before the blocks are harnessed together, while the remaining blocks might be insulated after they had been harnessed into train formation and transport operations had begun. This would allow more efficient use of insulating crews and equipment during the relatively long and slow movement in the Southern Ocean. One insulating crew plus equipment might consist of 8 to 12 men, two auxiliary ships (one on each of the submerging and emerging sides of the iceberg) for transporting

[1] Coriolis forces are caused by the earth's rotation. They tend to deflect an object moving in the Northern Hemisphere to the right and one moving in the Southern Hemisphere to the left of the desired direction of motion.

and engaging the rolls of insulation, and topside equipment for winching and cinching the laps of insulation. Three crews would probably be required to keep one set of equipment operating continuously, with crews being changed and equipment being resupplied every 8 hours (the launches could be interchanged at midtime lunch intermissions in order to make additional rolls of insulation available).

Harnessing an iceberg would require an encircling cable and net assembly primarily below the water line, but with topside suspension. A sling network could be underlaid with tough plastic fabrics near points of greatest pressure against the icebergs. This would distribute the load over most of the surface area and prevent serious ice cutting or harness sliding with varying or uneven application of thrust forces.

Some above-water preparation of the iceberg, particularly near soft sharp topside edges, would help with the topside insulation operations and harness suspension. This may require special chipping equipment operating from the topside. Cable-attached blades pulled over the topside by a cable between tugs on each side of the iceberg might also be quite useful. Suitable methods of preparation should evolve from experience which could make the preparation much less costly in time and materials than insulating the icebergs. The topside preparation of the icebergs and their insulation and harnessing should also greatly reduce the calving and erosion that would be experienced in iceberg transit through warm stormy waters.

It should be possible to select icebergs without serious fault planes or structural weaknesses from the predominantly sound, natural tabular configurations that are available. Iceberg thickness will determine whether icebergs can withstand breakup, as opposed to edge erosion, in the heavy seas that will be experienced. Preliminary estimates indicate that a 100 m thickness of solid ice (below any loosely packed snow on top) should provide an adequate strength margin against the stresses from the largest wind-wave systems that might be encountered. If longer wave-length systems such as tsunamis[2] were encountered with characteristics that exceed the breaking stress of the icebergs, the icebergs would tend to break into lengths greater than the thickness so as to remain stable in flotation. The train harness system should be designed to adapt and contain the "pieces" in the same general train configuration without serious effect on the transport operations.

TRANSPORTING ICEBERGS AND CONTROLLING MELTING

The transporting of fresh water from the Antarctic *in the form of iceberg trains* rather than converting it for more conventional shipment seems to be especially attractive. The Antarctic is readily accessible to the world's oceans and is the only region with a potentially adequate continuous yield of tabular icebergs that can be harnessed into large enough trains to make the operations economically attractive. The ability to form these economically viable trains stems in part from the fact that conventional resistances to movement through water are proportional to the water-exposed surface areas, whereas the associated volume increases more rapidly than the exposed surface area so that the transport cost per unit of volume decreases with

[2] Sea waves of seismic origin.

increasing size. For the very large masses of icebergs that become economically attractive for transport at low speeds to the Northern Hemisphere, *the dominating contending resistance (except very near the equator) is the Coriolis force.* Transport operations should be designed to reduce Coriolis effects even at the expense of more conventional resistances.

In the design of large ships, the conventional limit to the achievable speed is the wavemaking resistance [28]. However, when operating at speeds well below the wavemaking barrier, the principal resistance for conventional ship designs is from skin friction, which might typically provide 0.8 of the total resistance. The form drag or eddy-making resistance can be designed to be a relatively small fraction of the total resistance. For motion along its length, the iceberg's resistance from the form drag and skin friction can be represented approximately by

$$D = \tfrac{1}{2} \rho V^2 [A_\ell C_D + A_\omega f_s] \tag{1}$$

where D = drag (newtons),
ρ = density of sea water (kg/m^3),
V = free stream velocity (m/s),
A_ℓ = maximum frontal area for determining form drag (m^2),
A_ω = wetted surface area for determining skin friction drag (m^2),
C_D = form drag coefficient,
f_s = skin friction drag coefficient.

Most tabular icebergs that are shaped by natural stress cleavage are more frequently found with rectangular shapes and blunt ends. As a consequence, the form drag is likely to dominate the skin friction for most icebergs. Large ships are designed with equivalent form drag coefficients, C_D (based on maximum frontal cross section), of 0.04 to 0.06. Specially selected ship-shaped or streamlined icebergs (both front and back) might yield a form drag coefficient of 0.1. However, a more casual selection of icebergs should be possible without exceeding coefficients of 0.2. Finally, the form drag coefficient for a rectangular iceberg in broadside motion should approach unity, whereas in longitudinal motion the corners should soon ablate to approach a drag coefficient of about 0.4. The form drag coefficient for a train of icebergs with streamlined leading and trailing units and with well-matched and abutted intermediate units should range between 0.2 and 0.6, depending on how the icebergs are joined together [29].

The skin friction coefficients, f_s, for icebergs based on wetted area are apt to range between 0.002 and 0.003, depending on, among other things, the streamline length and speed (see Appendix D). For the values of the coefficients of skin friction and form drag that have been indicated, and for iceberg configurations that we may wish to consider, the form drag is apt to dominate the skin friction by an order of magnitude if the iceberg length, L, is only a few times the width, W. However, if L/W $\simeq$ 30, the two resistances may be comparable, and if L/W $\simeq$ 300, the skin friction is likely to dominate the form drag by an order of magnitude. If an iceberg train is rectangular, except for rounding of the ends, and of fixed depth, the optimum value of L/W to minimize the combined form drag and skin friction resistance would be approximately $C_D/(2f_s)$. However, Coriolis forces and other factors are likely to place other constraints on the L/W that is chosen. For example, the width must be large

enough in comparison with the thickness so that an adequate margin of stability against rolling can be maintained throughout the transit. There may not be an adequate selection of icebergs with width values approaching the thickness. Iceberg trains are most likely to be selected with widths ranging between 300 and 1200 m and with thicknesses ranging between 150 and 300 m. (In some areas many icebergs appear to have characteristic widths of 400 to 600 m, which suggests that trains formed in these areas should harness icebergs with these widths.)

The optimum transport speeds are likely to be less than 1 m/sec (2 kn). At these speeds the wavemaking resistance can be neglected in comparison with other resistances. However, *at very low speeds the effects of Coriolis forces are likely to dominate design considerations and the costs of moving icebergs at high latitudes.* This introduces a design factor that has not previously been important for practical transport situations, and there are many unknowns that need to be explored for the design of efficient operational configurations. The classical Coriolis force on a mass moving on the earth's surface is approximately given by

$$F_c = 2\,MV_e\Omega \sin \phi, \tag{2}$$

where F_c = Coriolis force (newtons),
M = mass (kg),
V_e = velocity relative to the earth's surface (m/sec),
Ω = angular velocity of the earth (radians/sec), 7.29×10^{-5},
ϕ = earth's latitude of the mass position.

For a moving mass in the Southern Hemisphere, the Coriolis force is at right angles and to the left of the velocity vector; in the Northern Hemisphere it is to the right of the velocity vector. The main reason for the uncertainty regarding the effects of Coriolis forces is that the icebergs are floating in moving seawater, which is itself under the influence of Coriolis forces. It is generally accepted that any large-scale, steady-state, circulating ocean current not under horizontal stress by the atmosphere or land can be considered to be in geostrophic equilibrium, in which the surfaces of equal pressure slope to compensate for the Coriolis forces and thus maintain the equilibrium flow. If an iceberg is imbedded in this flow without a velocity relative to the water, it will be in equilibrium and move with the water. Thus the Coriolis effects that are of concern in iceberg transport operations are those that can be associated with the velocity relative to the water rather than the earth. This is the interpretation used in applying Eq. (2) to modeling the transport operations described in Appendix D.

A more important Coriolis factor of greater uncertainty is the counteracting effects of displaced water. If an iceberg is moving in the water, it is continuously displacing water from the front to the rear (see Appendix E), and the momentum of the displacing water with respect to the free stream is approximately equal and opposite to the iceberg momentum. Thus the Coriolis forces on the displacing water are approximately equal and opposite to those on the iceberg. The important question is, how much of the effects are cancelled?

As a first approximation for an iceberg with rectangular faces in water undisturbed by propulsion, the fraction of the displacing water that moves around the sides is about h/W, where h is the submerged depth and W is the width or beam,

and W > h. If the bow and stern are wedge shaped so that the water is separated to the sides, a larger fraction of the displacing water should move around the sides, whereas if the bow and stern are beveled toward the bottom, more of the displacing water should move under the iceberg. Also, if the iceberg is moved by propelling water near the sides (or bottom), the fraction of the displaced water moving with the propelled water should be increased. It is difficult to estimate the net effects of shaping and propulsion on the flow of displaced water. However, if the shaping and propulsion are selected to enhance the flow of displaced water around the sides rather than under the bottom, more of the direct Coriolis forces should be cancelled and the net Coriolis effects should be less than about (W − h)/W times the direct Coriolis force on the iceberg. The best iceberg width, W, to minimize Coriolis effects will usually be the smallest one that can be readily found that sufficiently exceeds the thickness in order to maintain roll stability and integrity against breakup during transit operations. In many cases it should be possible to select widths so that the net Coriolis forces are less than half of the theoretical direct Coriolis forces on the iceberg.

Another important aspect concerning Coriolis forces is the propelling angle of the iceberg train. A component of the propelling force must be used to compensate for Coriolis forces. This means that there will be a propelling angle with respect to the iceberg velocity, and "lift" can be obtained to counteract any otherwise uncompensated Coriolis forces. This compensation has been included in the calculations for first-order effects as described in Appendix D; however, there are shape and aspect-ratio uncertainties about lift coefficients for the configurations that may be involved. Since the lift is proportional to the velocity squared, V^2, while the Coriolis forces are proportional to V, the control and tow angle must be modified with changing velocity, and navigation through restricted passageways becomes quite complicated. However, a properly instrumented towing operation in which the tow angles are measured may offer a singular opportunity to determine many of the unknowns about Coriolis effects. Such tests seem highly desirable in order to design efficient operational transport systems.

The ocean currents and weather, including the winds and waves, will affect transport operations. However, it is very difficult to estimate their influence because their magnitudes and directions are so variable and the seasonally averaged statistical data are very poorly defined, sampled, and measured. The ocean current data principally involve surface currents as they influence conventional shipping. Icebergs with much deeper drafts would be influenced by deeper currents that might be quite different, particularly in the equatorial zone. The net difference averaged over a transit to the Northern Hemisphere is estimated to be the equivalent of a slight dampening of effects based on the surface currents and is not expected to be a significant factor in the assessment of operational feasibility.

The influence of the winds is of even greater uncertainty. The wide variation and distribution of magnitude and direction of winds in most areas and seasons make it difficult to properly estimate their effects from data of mean behavior. The average height of tabular icebergs projecting above water is adequate so that an average wind speed equal to the 10-m height value could be assumed to impinge on the icebergs without distorting the accuracy of the original data. The wind effects (drag and lift) could then be introduced in the computations in a manner very similar to the effects of motion relative to the water (see Appendix D). In our

trajectory computations, however, the treatment of wind effects was simplified by prescribing a straight-line course between pairs of points along the trajectory. If the winds for any fraction of the time in any segment of the trajectory proved too great for the propelling power to provide a resultant speed in the prescribed course direction, no computer solution would be obtained. The procedure probably denied solutions for smaller propelling powers, a problem that would be circumvented in practical operations by less rigid insistence on a prechosen course.

The effects of wind-driven currents, as distinguished from the statistical seasonal data on currents, were neglected in the computations. Any such effects are likely to be small in comparison with the direct wind effects. Wind-wave effects also were studied, but no quantitative influence was included in the computations. It seems clear that the icebergs will be so large compared with the largest waves that they will ride out the waves with very little rocking. Furthermore, they will act as very effective breakwaters and will almost totally reflect most waves. However, although the waves can carry enormous energy, they do not appear to transport a correspondingly large momentum to be reflected from the icebergs. Also, the run up or excess pressure produced by increased average water level on the wave side of a *fixed* vertical breakwater is not apt to manifest itself significantly against a *free-floating* iceberg. Since we could not obtain useful statistical data about wind waves along the trajectories of interest, and found no satisfactory way of quantitatively introducing the effects, their influence was not included in the trajectory computations. Even if their effects on transporting operations are comparable with those for the direct wind, the computer simulation of these operations indicated that there was no pronounced effect on transit times to Southern California, no matter whether the expected winds or no winds were encountered. Thus, although any practical transport operation must take into consideration many of the effects of wind waves, the waves are not expected to influence greatly the propelling power required.

In order to determine the sensitivity of transport operations to the many parameters involved and to establish a basis for interpolating or extrapolating the propelling power requirements, a computer program was devised to include the effects of the various parameters of interest. This work and the details of the results are included in Appendix D. Only a brief interpretation will be presented here.

Two routes were examined between the same terminals. The departing terminal was arbitrarily selected at 70°S latitude and 170°W longitude in the Ross Sea; the arriving terminal was Los Angeles. The long route (8,660 n mi) followed (and took advantage of) the Peru current along the west coast of South America in a traditional "sailing" route, and the short route (6,875 n mi) was more direct and cut across currents to merge with the longer route at 10°N and 111°W. The two routes are illustrated in Fig. 3, which shows the 5° latitude segments over which parameters were averaged in making the computations.

The sensitivities to currents and winds were tested by comparing the transit times for a long ice train (80 km $\times$ 600 m $\times$ 300 m $\approx 1.22 \times 10^{13}$ kg), which had a given propelling force (10^8 newtons) over each route under the expected current and wind conditions, with the transit times when either or both the currents and the winds were made zero. It was found that there was a slight increase in transit time (1.6 to 9 percent) when only the winds were made zero and with 1/2 maximum

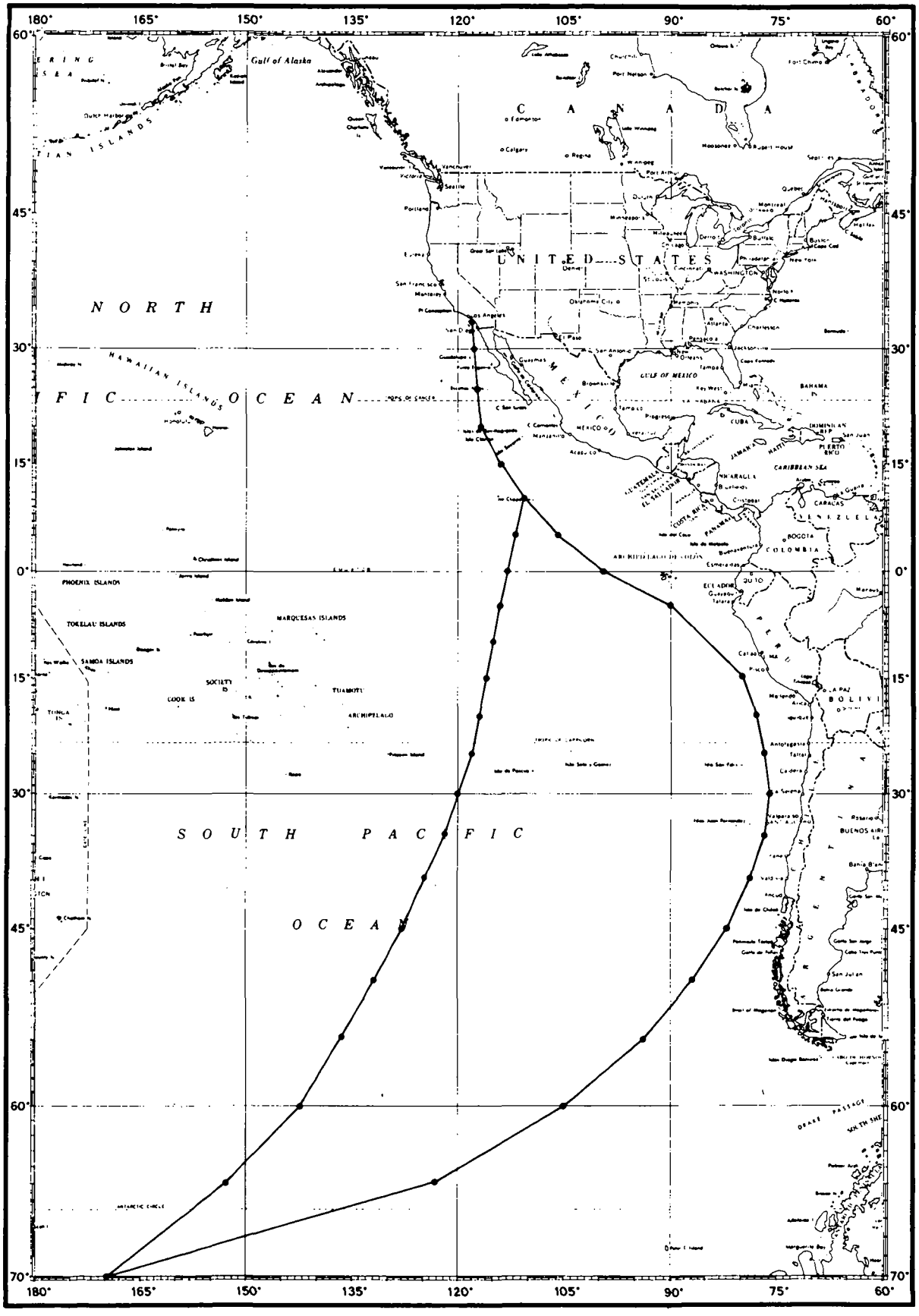

Fig. 3—Two routes from Antarctica to Southern California

direct Coriolis force; with zero effective Coriolis force, there was a slight decrease in transit time with zero wind. On the other hand, the currents had a greater influence. When only the currents were made zero, there was a 35 percent (long route) to 12 percent (short route) increase in transit time. When both currents and winds were made zero, there was a 37 percent (long route) to 20 percent (short route) increase in transit time. In comparing the two routes, the short route had 9 to 17 percent less transit time than the long route with the expected currents, and about 40 percent less transit time in the absence of currents. Thus the 26 percent longer route that was selected to take advantage of currents requires 40 percent greater transit time in the absence of currents and only 9 percent greater transit time for the expected currents and winds.

It appears that the more direct route between the two terminal points is the better one for transit times of about a year or less. However, given the expected transport conditions, the transit times do not appear to be very sensitive to a wide range of route possibilities. Also, the total transit times are not very sensitive to the average winds; below 30°S latitude, however, the wind influence can be significant if it happens to be consistently favorable or adverse. The 1-year transits were found to be relatively insensitive to environmental factors, because the required propelling forces were large in order to overcome Coriolis effects. For a 2-year transit, the velocities and Coriolis force would be significantly reduced, and so the propelling force would have much greater competition from fluctuating environmental factors causing the total transit times to become much more uncertain.

The transit-time sensitivity to the length-to-width ratio of an iceberg train was tested for a given mass (1.22×10^{13} kg). Lengths of 80 km, 40 km, and 20 km, and corresponding widths of 600 m, 1200 m, and 2400 m were tried with reduced form drag coefficient (C_D) values for the wider cases in order to increase the improvement for the form drag and skin friction. However, the Coriolis forces (at one-half of the maximum direct Coriolis force on the iceberg) were so dominant that the longest and narrowest configuration with the greatest lift benefit proved to be significantly better even though the others provided shorter transit times within 15° of the equator where Coriolis forces are suppressed.

The propelling force and transit time were tested to determine the sensitivity to size (or length) of iceberg train for a fixed width (600 m) and thickness (300 m) over the short route. The 80 km train with a tow force of 10^8 newtons and a C_D of 0.6 had an 8 percent shorter transit time than the 8 km train with a propelling force of 10^7 newtons and a C_D of 0.1. This indicates that the form drag with an optimistic $C_D = 0.1$ still has significant influence at 8 km length. However, no significant improvement in propelling force per unit mass is expected for trains longer than about 20 km. A train that is 0.8 km long with a propelling force of 5×10^6 newtons was unable to negotiate the equatorial currents on the route, indicating a sort of propelling-force threshold required to complete a transit no matter how short the "train" is made. For trains of a given width and thickness, the costs in terms of propelling energy, harnessing, and insulation should become proportional to the length beyond about 20 km, for widths of about 600 m. Thus the transport cost per unit of ice will approach its lowest-value asymptote at this point, and the decreasing energy cost per unit with increasing power-plant size is the only further cost advan-

tage to increasing the length of the train. However, this asymptotic cost value depends on the width and thickness of the train and the trade-offs between energy, insulation, and harness costs as functions of width and thickness. The cost per unit is likely to be the least for the narrowest train that can be formed from readily available icebergs. This is estimated to be for widths between 300 and 600 m.

The asymptotically best configuration for a 1-year transport cycle over the illustrated routes leads to a ratio of propelling force to iceberg mass of approximately 8×10^{-6} m/sec^2. Since any acceleration will also involve an equal mass of displaced water, the effective inertia of the system will limit the maximum accelerations to approximately 4×10^{-6} m/sec^2, and a few days (or a few train lengths) will be required to make significant changes in speed or direction in transit when most of the available forces are used to overcome noninertial resistances. This sluggishness means that control should be preprogrammed with the best available information about the specific ice train parameters and the environmental factors. A suitable computing progam for operational control will be required to take into account the inertial and fluctuating environmental factors. Such a program would be essential for any practical operation, but it would not be expected to produce significantly different transit times for a given train configuration compared with the transit times that were derived with the computations that did not consider accelerations over prescribed courses.

In Appendix D, an approximate graphical solution of the transport equations is developed that is useful for providing preliminary estimates in the absence of currents and winds. This solution gives the transport speed (and propelling angle) as a function of latitude, iceberg size and shape, drag and lift coefficients, and propelling force.

The propelling power required to provide a given propelling force depends on many configuration details. However, more efficient use of power can generally be achieved by increasing the area engaged by the propeller systems. Appendix D gives estimates of horsepower for propelling force with reasonable assumptions about configuration details. As an example, it indicates that a propelling force of 10^8 newtons could be provided with 1.35×10^6 horsepower (~10^6 kW) applied to 16 propellers, which are each 36 ft in diameter. This value is used in estimating the asymptotic energy costs for delivering iceberg trains.

The melting rates of an unprotected iceberg depend upon the local heat-transfer coefficients and the water and ice temperatures. Thus the rate will vary along the length of the iceberg as is indicated in Appendix B, and with depth changes in ocean water temperature. The actual melting rates can only be determined very crudely with the available information. However, it is clear that more than a 1000 m depth of ice would melt from an unprotected water-exposed ice surface in transit to the Northern Hemisphere at any reasonable transit speed. Thus it is essential to insulate ice surfaces from seawater ablation for transport to the Northern Hemisphere, and it will probably also be economically attractive for shorter transits to the Southern Hemisphere. As previously discussed, the most attractive way so far conceived for insulating icebergs is to trap a quilting of melt water between the ice and the seawater boundary layer by means of thin films. By confining the melt water to small enough pockets so as to inhibit convection, the heat transfer is primarily limited to *conduction* through the melt-water quilt. As is indicated in Appendix B, under these conditions, 2 to 3 cm of water-quilt thickness should limit the melting

to less than 10 percent in a 1-year transit. It should be possible to achieve such protection in a variety of ways. The selection of good operational techniques will require testing in the operational environment. The design goal will most likely be to use the minimum film that will insure satisfactory performance for one trip, after which the film can be appropriately disposed. It is estimated that a total film strength equivalent to less than 25 μm of Mylar will be required for satisfactory protection.

The estimated costs of delivering icebergs to terminals for the asymptotic 1-year cycle are developed in Appendix C. It appears that this could be accomplished for about \$8 per k•m^3 (\$10 per acre-ft) for iceberg trains of about 3×10^6 acre-ft or larger. This cost is not expected to vary very much with transport distance unless the power supply can be gainfully used near the terminal to help provide revenue for capital investment return during any waiting period. Eventually, the ideal situation might be one in which a standard interchangeable power supply system of, say, 10^6 kW(e) is used everywhere for electrical supply, and from which the excess capacity at any time could be used or stored in convenient form (e.g., hydrogen, oxygen, and minerals from electrolysis of ocean water). With such a multipurpose system, the optimum towing speed for minimum total cost (fuel, capital recovery, operating expenses, etc.) could be used, and the icebergs could still be acquired on a yearly cycle. This would enable the asymptotic costs to be reduced, particularly for the shorter hauls, e.g., to Australia. However, the costs per unit of delivered ice are not apt to be reducible by more than about 20 percent with such methods, and the estimated iceberg delivery costs are already only a minor factor in the total systems cost and concept feasibility. Thus it does not appear to be important to pursue such refinements at this point in the assessment of concept feasibility.

TERMINAL CONVERSION FOR FRESH WATER AND HEAT SINK

The terminal conversion of icebergs into fresh water or heat sink is an essential feature of any concept for using iceberg resources. This phase of iceberg exploitation is likely to involve a major portion of total exploitation costs, and promises large returns for innovative techniques and concepts that are less costly and more beneficial to the environment. Preliminary indications are that heat to melt the ice might best be obtained by heat exchange with the ambient seawater environment and with the thermal discharges from electrical power generation and other industries. The principal problem is to achieve the required melting rates with a minimum expenditure of artificial mechanical energy.

If the conversion of ice to water is accomplished by melting through heat exchange with ambient sea water, a number of heat transfer steps in series will limit the rate of heat flow and the melting. The ice is melted by the ablative transfer of heat from the melt bath, which is convectively heated from the barrier wall separating the seawater from the fresh water melt. The warm seawater convectively transfers heat to the wall barrier, which conducts it to the fresh water side. In order to increase melting rates, the exposed surface areas of ice and wall barrier, as well as the convective movements of the waters, can be increased. The heat exchange can be achieved by moving the ice and melt through pipes immersed in ambient seawa-

ter currents, or by containing the ice and melt in shallow flexible membrane barges with large barrier areas, using surface wave and tidal action to stir up greater convective heat transfer.

Melting of ice with the aid of low-grade waste heat from electrical power generation offers the attractive benefit of improving the efficiency of generating power if an intimate connection can be made with the power-plant cooling water system. The waste heat from a 10,000 MW(e) power-plant complex could melt about one million acre-ft of water-equivalent ice in 1 year. The most likely connection will be made by pumping an ice slurry to the power-plant vicinity rather than establishing a pumping loop from the power plant to a conversion site in the ocean. With present power-plant sizes, the available waste heat at any one site is small compared with the energy rate required to melt several million acre-ft of ice per year. Thus, unless major changes take place in the size of power plants, the direct use of waste heat will not be a major factor in the economics of converting icebergs to water. Instead, heat exchange with ambient seawater will be the dominant mode for supplying the energy for melting.

The greatest energy consumption in the conversion process is likely to be in the cutting or breaking of the ice to form small enough volume-to-surface-area ratios to achieve the melting-rate objectives required. Four general methods have been conceived for cutting ice, each of which may have advantages in different situations. Listed in the most likely order of efficiency (in terms of increasing relative work needed for application), these are:

- Splitting, cleaving, shearing, or chipping without forming a kerf.
- Ablating a kerf by convective heat transfer with pumped water.
- Sawing, drilling, or mechanically chipping a kerf.
- Melting a kerf by the direct application of heat energy.

The first method (splitting) will normally be much more efficient than the others because it forms a minimum kerf and new free surface area, even though it may require larger forces than are available in some situations. However, it should remain an attractive alternative for partitioning icebergs regardless of the size of the cross-section cut that is used, from the largest ones requiring millions of square meters in cross-section to the smallest ones involving less than 1 m^2 of cross-section. There may be an opportunity to directly exploit the otherwise dissipated sea-wave energy to operate an "ice crusher" to break up the larger ice chunks and to stir the ice-bath mixture, with very little other energy required. This should be an attractive way to use wave energy rather than letting it just dissipate in shore erosion.

The ablation of a kerf with warm ambient seawater is likely to be of most interest in warm terminal areas or while crossing tropical waters. This method is mechanically most efficient when the warm ambient seawater is pumped or moved slowly to cut the kerf. This procedure might require less mechanical energy than 1 percent of the heat energy for melting the same kerf. The direct-melting method would then not be of much interest unless a much smaller kerf could be used, and this may not be possible or desirable in many applications. Thus the ablating method may become attractive outside of the Antarctic for widely spaced cuts for which the relatively wide ablation kerfs are still only a small fraction of the total ice volume, and for situations in which the splitting method cannot easily be applied.

The mechanical energy of chipping a kerf will in many situations be the equivalent of *melting* the kerf. However, if this method can be applied so that the kerf chips are ejected with the immediate melting of only a small fraction, and if the kerf can be made a few tenths of a percent or less of the total ice, it may become an especially attractive method to use in the Antarctic and in situations where high cutting speeds are important.

The least efficient use of energy for cutting (the direct melting of a kerf) can still be a much more efficient method of converting ice to fresh water than the direct melting of all the ice, since the kerfs that are required can be made only a small fraction of the total ice volume to be converted.

Only a very rough preliminary estimate of conversion costs can be made without an engineering study and comparison of systems that could be derived from the various techniques that have been described. It is estimated that cutting and moving can be achieved with less energy than 1/300 of the heat of fusion (systems would be designed to produce kerfs less than 1/300 of the volume) or about \$2 per $k \cdot m^3$. The requirements for labor (other than for power generation) are estimated at about \$2 per $k \cdot m^3$ for the highly automated operations. The amortized cost of capital investment, including maintenance and insurance at an annual rate of 1/10 of the initial investment, is estimated, by comparison with analogous operations, to be two to three times the energy costs. Thus, the total conversion costs to provide fresh ice water at the seashore is estimated to be about \$8 per $k \cdot m^3$ (\$10 per acre-ft). For a typical installation with a capacity of 3×10^6 $k \cdot m^3$ per year, this would mean a capital investment of perhaps \$200 million, exclusive of the power-generating equipment.

In order to lift the water from seashore level and carry it inland to wholesale distribution terminals, the added cost per $k \cdot m^3$ would be about \$8 per 300 m of lift plus a few dollars for transporting the water a few tens of kilometers at capacities of 1 to 10×10^6 $k \cdot m^3$ per year, depending on the specific terminal configuration and environment.

Once the ice has been melted, the melt water can be blended with other water or processed in other appropriate ways for fresh water uses. The ice water can also be pumped to suitable locations for use as a heat sink and to abate thermal pollution before it is used for other fresh water purposes. The potential uses of the melt water, particularly as a heat sink, are best explored in the context of specific terminal-using environments.

IV. ASSESSMENT OF SOCIETAL AND ENVIRONMENTAL IMPACTS

INTERNATIONAL ACCEPTABILITY OF EXPLOITATION OF ANTARCTIC ICE

There does not appear to be anything in the harvesting of ice from the Antarctic that is basically in conflict with the Antarctic Treaty[1], as long as the environment is properly protected. However, before large-scale operations are undertaken it would seem appropriate to organize a planning conference for all concerned nations in order to arrive at an agreement about rules of harvesting that would ensure protection of the environment and opportunities for all to share in the benefits. There is no currently known technological obstacle that would preclude such an agreement or present an insurmountable economic barrier. However, the planning conference for such an agreement would need more detailed descriptions and definitions of the potential operations in order to have a basis for establishing the rules of harvesting. As long as the demand for ice resources remains only a small fraction of the annual yield, the rules of exploitation need not significantly increase the systems costs nor threaten the Antarctic environment. When the demand approaches the annual yield, the rules required for more efficient harvesting may increase the costs and could conceivably influence the environment. The planning conference should develop harvesting rules that could evolve gracefully to cope with the eventual situation when the demand approaches the annual harvestable yield.

EN ROUTE ENVIRONMENTAL CONSTRAINTS

The en route environment will depend on the route selected to satisfy time and energy constraints, which are influenced by transit speeds, Coriolis forces, currents, winds and waves, temperatures, oceanic depth limitations, and other land or marine interference. Oceanic depths will limit applications for areas around most of the

[1] Signed by the following on December 1, 1959: Argentina, Australia, Belgium, Chile, the French Republic, Japan, New Zealand, Norway, the Union of South Africa, the Union of Soviet Socialist Republics, the United Kingdom of Great Britain and Northern Ireland, and the United States of America. It was drafted, as stated in the preamble, in recognition "... that it is in the interest of all mankind that Antarctica shall continue forever to be used exclusively for peaceful purposes and shall not become the scene or object of international discord."

Gulf of Mexico, the east coasts of North and South America, Western Europe, Eastern Asia, Indonesia, the Persian Gulf, and many arid parts of the world. For example, one potentially interesting destination involving passage through the Red Sea to the Gulf of Aqaba would require clearing the brief deep water obstruction in the southern Red Sea, and would call for special navigation control through narrow passes under the influence of Coriolis forces. Similar situations exist in parts of the Mediterranean and other restricted passageways around the world. However, there should be no serious depth or navigation limitation problems in reaching most of the west coasts of North or South America, including the Gulf of California, nor much of Australia that might be of interest.

Route selection will be based on the influence of the many factors that determine the cost of transport, but the selection must also take into account the possibility of interfering with shipping, fishing, and other maritime activity. Each terminal destination will involve a different set of considerations for route selection and en route environmental protection. However, no serious or costly constraints on operations have yet been uncovered that would impose unacceptable demands for the protection of the en route environment.

ACCEPTABILITY OF TERMINAL OPERATIONS

The environmental impact of the terminal operations and the acceptance by the public and special interest groups may prove to be very important in the concept feasibility for any specific terminal area. These factors can be assessed when proposed terminal operations are better defined and can be related to a specific terminal area. The terminal operations would involve large installations that could be expected to modify activities along any highly developed coastal region. An iceberg train tens of kilometers long tethered against the ocean bottom 5 to 10 km from shore would serve as a huge breakwater to tame the inland sea and make it locally unattractive for surfers. The local waters would be cooled slightly since there would be more than enough ice water to compensate for "hot" thermal pollution. However, in most areas the "cold" thermal pollution would quickly disperse so as to make only minor modifications in the seasonally varying temperatures or produce the equivalent temperature effect of a small change in latitude (probably less than one degree in most situations). The local effects on marine life would have to be explored for each situation. If it could be measured, the durations of migrations and the types of marine life encountered are likely to be modified as would be expected with a small change in latitude.

The weather, aside from a small local change in temperature, should not be greatly modified, unless the terminal is in a transitional region for fog production, in which case it is conceivable that the local fog statistics might be altered somewhat. Thus, the effects on weather and marine life may be difficult to discern, but each proposed terminal operation would need to be investigated in detail to determine what effects to expect. Public acceptance of the sight of the operations and the land use along the shore would also have to be explored at each location. In some cases there might be some opposition to any operation that would support or benefit development and population growth in an area. Such opposition is most likely to delay development, make it more costly, and limit the benefits that might accrue.

INTRODUCING NEW WATER RESOURCES

In most systems for using water, a major portion of the investment cost is used for developing the system and processing and distributing the water. The costs of developing population, industry, or agriculture in an undeveloped area are likely to be large compared with the costs of obtaining water, and therefore the development costs will usually pace the demand for water. Since iceberg water becomes more economically attractive when used in large quantities (e.g., millions of acre-ft per year), its earliest demand should come from large developed water users for which the icebergs appear as an attractive alternative new water supply. The processing and distribution systems already in use would be continued wherever possible, and old sources of water might be kept accessible for emergency and reserve use.

The demand for water that might be generated from a large development can be illustrated with the area around the lower Colorado River (principally Arizona, Southern California, and the bordering areas in Mexico). The "Lower Colorado Region," defined to include primarily Arizona and only small parts of bordering Utah, Nevada, and New Mexico, has a current annual water consumption of about 6 million acre-ft and a projected consumption of more than 8 million acre-ft by the year 2020 [30]. The local water supply, including the entitlement from the Colorado River that is used, is only about 4 million acre-ft annually. The difference must be provided by ground water overdraft, water importation, or the equivalent of Colorado River augmentation. The ground water overdraft is lowering the water table, increasing the water cost, and degrading its quality. A rescue operation to provide 2 to 4 million acre-ft of additional water supply is needed to maintain the current conservative land use. Most of the water consumption (5 to 6 million acre-ft per year) is for irrigation of 1.8 million acres of cropland from a total suitable and available cropland of 16.8 million acres. If crop demand would warrant it, an additional 15 million acres of crops requiring 50 to 75 million acre-ft of additional water annually could be developed.

To augment its own supply, Southern California imports water from Northern California and also draws about 5 million acre-ft per year (4.4 million acre-ft per year assured after other entitlements have been exercised) from the lower Colorado River. About 4 million acre-ft per year of the Colorado River water is for long-established irrigation use, principally for the Imperial Irrigation District. If there is no expansion of irrigation, most of the projected increases in water usage for Southern California for at least the next 30 years could be satisfied by the California State Water Project, although the real costs (by meter and taxes) are much too high to be attractive for most agriculture.

The Metropolitan Water District of Southern California currently draws 1.2 million acre-ft per year from the Colorado River Aqueduct. This is the longest and most expensive westward diversion of Colorado River water. Perhaps if the Colorado River Aqueduct could be reversed to carry iceberg water to the Colorado, this might prove to be an attractive way of augmenting the Colorado. Additional augmentation might involve substituting iceberg water for westward diversions of the Colorado for irrigation purposes, or to directly satisfy the Mexican treaty entitlement from the Colorado River. In any event, there are many ways of using highly developed water distribution systems in the Pacific Southwest to quickly absorb many millions of acre-ft of iceberg water and to satisfy latent demands for high-quality water at attractive prices.

In many less-developed parts of the world, the investment burden for the development of water use and the exploitation of Antarctic iceberg resources may be too great to quickly assert latent demands. Thus, the worldwide demand for Antarctic ice water should exhibit an orderly growth for many years before the adequacy of the supply should significantly increase the cost.

ICEBERGS AS RESERVOIRS AND RECREATION AREAS

Reservoirs are important components of any water system. They store the surges of water that become available from natural sources, and therefore limit the flood losses and reserve a continuous water supply to satisfy the needs as they develop. Ideally, an adequate reservoir capacity for meeting the needs of an area over a number of lean precipitation years is desired. However, when the total water supply is already marginal, an adequate conventional surface reservoir capacity may lead to evaporation losses that significantly reduce the total supply. Icebergs might serve as better reservoirs since they should suffer little or no evaporation loss. In fact, there may be a net gain in fresh water averaged over a year due to condensation from the atmosphere. Furthermore, iceberg reservoirs need not displace valuable land or other resource use, and they might be developed and used in many imaginative ways as readily accessible ice recreation areas. The icebergs could be made less vulnerable to natural (e.g., earthquake) or man-made (e.g., bombs or pollution) catastrophes, and less hazardous for collateral losses of life and property. They could be moved or changed as the needs develop, and they would not require as great a capital investment or resource commitment or denial as more conventional reservoirs. The greatest loss problem of iceberg reservoirs is water lost to the saltwater environment. It will be very difficult to recover most of the final iceberg melt and exclude unwanted seawater pollution. A variety of techniques and concepts for using icebergs as reservoirs and recreation areas needs to be developed that can be adapted to meet the needs of the various potential terminal areas.

RISK IN ICEBERG-WATER RESOURCE SYSTEMS

Unless an integrated water system has adequate reserves (e.g., adequate underground aquifers) or alternative water resources that could satisfy minimum requirements for at least one year, the potential users are not likely to risk being dependent on a single source for an uninterrupted supply of water. However, systems that could maintain fully charged underground aquifers and alternative sources of water supply that could quickly adapt to the interruption of a principal water supply might find the addition of high-quality iceberg water resources very desirable. On the other hand, undeveloped arid regions without satisfactory underground or other reservoirs or alternative sources of water would need to develop acceptable redundancy or flexibility with iceberg water resources before they could risk much development that was dependent on uninterrupted water service. The cost of providing the needed dependability may become a feasibility barrier, but this depends on the particular

area to be served. However, there are many areas, including Southern California, where system risk need not threaten the concept feasibility. This factor must be assessed independently for each terminal area as the concept and options become better defined.

Appendix A

ICE ACCUMULATION AND LOSS IN THE ANTARCTIC

The rate of accumulation of ice in the Antarctic from atmospheric precipitation has become reasonably well established, and the values indicated in the Antarctic Atlas [22] will be used to illustrate a more detailed mass balance in the Ross and Ronne-Filchner catchments. The Ross catchment can be divided into three portions:

- The Ross Shelf with an area of 53.8×10^{10} m^2 and responsible for an average catchment of 0.10×10^{15} kg/yr.
- The East Antarctic catchment portion with an area of 112×10^{10} m^2 and responsible for an average catchment of 0.11×10^{15} kg/yr.
- The West Antarctic catchment portion with an area of 66×10^{10} m^2 and responsible for an average catchment of 0.12×10^{15} kg/yr.

Thus the total Ross catchment area of 232×10^{10} m^2 collects an average of 0.33×10^{15} kg of precipitation each year.

Similarly, the eastern portion of the Ronne-Filchner catchment of 200×10^{10} m^2 collects 0.20×10^{15} kg/yr, which could escape through the 175-km-wide throat east of Berkner Island; the western portion of 92×10^{10} m^2 collects 0.25×10^{15} kg/yr, which could escape through the 450-km-wide throat west of Berkner Island. Thus the total Ronne-Filchner catchment of 292×10^{10} m^2 collects an average of 0.45×10^{15} kg/yr.

The total area of Antarctica including its ice shelves is 1397.5×10^{10} m^2. If the average accumulation is 17 cm of water equivalent, this amounts to approximately 2.4×10^{15} kg/yr [22].

The principal loss mechanisms that need to be considered include:

- Calving or discharge of icebergs primarily from the outward flowing ice shelves and ice streams.
- Bottom melting primarily under the ice shelves but also under the grounded ice sheet and streams.
- Topside ablation, which is already accounted for in the net accumulation.

The loss from iceberg discharge can be estimated from the measured rates of ice flow in the ice shelves and streams. The loss from bottom melting can be estimated from temperature profiles near the bottom and mass balances along the flow. However, it is difficult to derive the appropriate heat flow for melting rates that would keep the total mass accumulation in approximate balance with the total loss. The tidal breathing under the ice shelves can be thought of as supporting the required heat flow by convective means without exceeding the measured temperature limits of the convecting seawater.

To illustrate the flows involved, consider the Ross Ice Shelf, which fluctuates and flexes about one meter between tidal extremes. The area of the Ross Ice Shelf is about 5.4×10^{11} m^2, so the quantity of water inhaled or exhaled under the shelf in 12 hours between tidal extremes is about 5.4×10^{11} m^3. The flow-limiting throat beneath the ice near the sea edge of the shelf has a cross section ($\sim$750 km $\times$ 310 m) of approximately 2.3×10^{8} m^2 [22]. Therefore, the average rate of tidal-water flow through the throat during these tidal periods is approximately 0.05 m/sec. Although the total one-way displacement of tidal water may be only a few kilometers, the turbulent boundary-layer growth from the ice bottom (down) and the seawater bottom (up) should provide a mechanism for enhancing the convective heat flow to account for the estimated melting from the bottom of the ice shelf.

The data available about the Ross Ice Shelf are sufficient to pro-

vide some confidence about the estimated loss mechanisms. However, data on the Ronne-Filchner Ice Shelves and most of the smaller, narrow ice shelves are inadequate to determine whether the mechanisms as extrapolated from the Ross Ice Shelf are consistent with actual losses. The estimated losses from the iceberg discharge and melt that are consistent with an approximate balance between accumulation and loss and the known data in the Antarctic are given in Table A-1. The estimated losses from the deep ice shelves (Ross, Ronne-Filchner) are predominantly from melt ($\sim$0.7), while those from the shallow ice shelves and direct glacier streams are principally from icebergs ($\sim$0.6). The total Antarctic losses are estimated to be nearly equally divided between melt and icebergs. Of course, all the loss is eventually in the form of melt, but for the purposes of Table A-1, the melt loss indicates only the melt from attached ice flow and does not include the melt from detached icebergs even if they are locked in fast ice.

Table A-1

ICE ACCUMULATION AND LOSS IN THE ANTARCTIC

	Catchment		Discharge	
Loss Mode to Sea	Area ($\times 10^{10}$ m^2)	Mass ($\times 10^{15}$ kg/yr)	Melt ($\times 10^{15}$ kg/yr)	Icebergs ($\times 10^{15}$ kg/yr)
Ross Ice Shelf (54×10^{10} m^2)	232	0.33	0.23[a]	0.10
Ronne-Filchner Ice Shelves (48×10^{10} m^2)	292	0.45	0.33[b]	0.12
All other ice shelves (56×10^{10} m^2)	873.5	1.62	0.44[c]	0.74
Direct glacier streams			0.10	0.22
Ice sheet			0.10	0.02
Total	1397.5	2.40	1.20	1.20

[a]Average melt rate, back of throat = 0.36 m/yr.

[b]Average melt rate, back of throat = 0.5 m/yr (tidal extremes twice the magnitude and twice the frequency of those at Ross).

[c]Average melt rate over bottom = 0.9 m/yr.

Appendix B

CONTROLLING THE MELTING OF ICEBERGS

The melting rates depend upon the local heat transfer coefficient and thus vary from one point to another along the length of the iceberg. The heat transfer rates are described differently for two regions of the iceberg train: a laminar regime, which lies within about 12 m of a bow stagnation point, and a turbulent regime elsewhere. The iceberg model is assumed to have a rounded bow characterized by a radius of curvature of about 250 m in both the horizontal and vertical planes. This curvature radius, comparable to the submerged depth, is an assumed first approximation to the shape acquired after the leading edges and corners have been removed by melting.

For potential flow around a fully submerged sphere, the tangential velocity is (3/2) V sin α; α is the polar angle measured from the leading stagnation point, and V is the speed of the sphere relative to the undisturbed water [31].

In the region of small α, the tangential speed is approximately

$$U = \frac{3VS}{2R} ,$$

where S = arc distance from the stagnation point, and R = radius of curvature.

For laminar flow, the heat transfer rate in such a region is constant and is given by[1]

$$h = 0.93k \left(\frac{V}{R\nu} \right)^{\frac{1}{2}} p^{0.4} , \qquad \text{(B-1)}$$

[1] See Ref. 32, Eqs. 10-22, p. 211 and subsequent comments.

where k = thermal conductivity of water, and ν = kinetic viscosity. For water at 10°C, $\nu = 1.38 \times 10^{-6}$ m^2/sec, k = 0.1388 cal/m-sec-°C, P = the Prandtl number ≃ 9.9, and with R = 250 m and V = 0.5 m/sec, the value of h is about 12.3 cal/m^2-sec-°C.

The region of laminar flow and constant heat transfer rate will persist to a Reynolds number (based upon S) of about 3×10^5. Using the potential flow approximation for small α, the distance S at the transition to a turbulent boundary layer will occur at

$$S = \left(\frac{2}{3} \cdot \frac{3 \times 10^5 \cdot R\nu}{V} \right)^{\frac{1}{2}} .$$

At 10°C with R = 250 m and V = 0.5 m/sec, it is found that S ≃ 12 m.

For S > 10 m, the Reynolds number will be given by

$$R_e = \frac{SU}{\nu} , \qquad U = \frac{3}{2} V \sin \left(\frac{S}{R}\right) ,$$

and the heat transfer coefficient[2]

$$\frac{h}{C\rho U} = S_T = \frac{0.0295/R_e^{0.1}}{A + R_e^{0.1}} . \qquad \text{(B-2)}$$

The number A depends upon the Prandtl number, but at 10°C, it is about 9.55.

Equation (B-2) is valid up to the point S/R = π/2, which for R = 250 m occurs at S ≃ 393 m from the stagnation point and is coincident with the joining of the rounded bow with the flat planes of the iceberg side and bottom surfaces. Values for h in this intervening region are given in Table B-1. These again apply to 10°C with the previously used parameters and where ρC = the volumetric heat capacity of seawater, 1.026×10^6 cal/m^3-°C.

---

[2]Ref. 32, p. 239, Eq. 11-9.

Table B-1

HEAT TRANSFER RATES NEAR THE ICEBERG BOW

S[a]	U[b]	R_e	S_τ	h[c]
12	0.036	3.13×10^5	6.37×10^{-4}	23.5
50	0.149	5.40×10^6	4.39×10^{-4}	67.0
100	0.292	2.12×10^7	3.65×10^{-4}	109.2
150	0.424	4.61×10^7	3.28×10^{-4}	142.5
200	0.538	7.80×10^8	3.06×10^{-4}	168.5
250	0.632	1.15×10^8	2.89×10^{-4}	187.5
300	0.700	1.52×10^8	2.78×10^{-4}	200
350	0.740	1.88×10^8	2.71×10^{-4}	206
393	0.750	2.14×10^8	2.65×10^{-4}	204

[a] In meters.

[b] In m/sec.

[c] The film coefficient, h, in cal/m^2-sec-°C.

For values of S greater than 393 m, the speed will be constant at 3V/2, and the film coefficient will gradually decrease as the Stanton number, S_τ, declines. Thus the maximum heat transfer rate is estimated to be about 206 cal/m^2-sec-°C.

The heat transfer rate depends upon the speed. The maximum rates (at S = 350 m) for several speeds are shown in Table B-2.

Table B-2

MAXIMUM FILM COEFFICIENT VERSUS SPEED

Speed			
m/sec	kn	S_τ	h
0.25	0.485	2.97×10^{-4}	113
0.50	0.97	2.71×10^{-4}	206
1.00	1.94	2.45×10^{-4}	370

The gradual decline of the heat transfer rate with increasing distance from the iceberg bow is illustrated in Table B-3.

Table B-3

HEAT TRANSFER RATES ALONG THE ICEBERG LENGTH

S	R_e	S_T	h
2,000	1.09×10^{9}	2.10×10^{-4}	162
4,000	2.17×10^{9}	1.90×10^{-4}	146
8,000	4.35×10^{9}	1.71×10^{-4}	132
20,000	1.09×10^{10}	1.49×10^{-4}	110
40,000	2.17×10^{10}	1.34×10^{-4}	103
80,000	4.35×10^{10}	1.20×10^{-4}	93

The units in Table B-3 are the same as in Table B-1; the local speed, U, is 0.75 m/sec for all values of S.

Melting rates are based upon a volumetric heat of fusion of 72×10^{6} cal/m^3. The melt rate in m/hr-°C is given by

$$\text{melt rate} = \frac{3600 \cdot h}{72 \times 10^{6}} \text{ m/hr-°C} .$$

It is somewhat more convenient to refer to melt in meters/nautical mile-°C, a number which is only weakly dependent upon the speed with which the mile is traversed. For the speeds given in Table B-2, the corresponding melt per nautical mile is given below in Table B-4.

As an example, the path length along the short route is 6875 n mi and the distance-averaged ocean temperature along that route is 17.8°C. The expected melt at a transit speed of 0.97 kn is about 1300 m.

The preceding example is somewhat inaccurate in combining speed relative to existing currents, and distances relative to the surface of the earth. In view of the extreme loss, which is greatly in excess of the thicknesses under consideration, the error due to this inaccuracy

Table B-4

MELT PER NAUTICAL MILE VERSUS SPEED

Speed			
m/sec	kn	h	melt/n mi-°C
0.25	0.485	113	0.0117
0.50	0.97	206	0.0106
1.00	1.94	370	0.0095

is rather unimportant. The clear result of the example is that insulation will be required if icebergs are to be brought to the Northern Hemisphere.

The insulation requirements can be specified in terms of the melt loss that can be tolerated. Thus if a 10 percent loss (30 m) can be tolerated, the effective heat transfer coefficient must be reduced from 206 cal/m^2-sec-°C to 4.75 cal/m^2-sec-°C. Almost the entire burden of the thermal resistance problem falls into the insulation domain, and the computation of losses becomes quite insensitive to the turbulent film theory described in the preceding paragraphs. In fact, if a net yield of 90 percent or better is required, the simplest procedure is to take no credit for the film coefficient, assume it to be infinite, and depend entirely upon the insulation for controlling the melting.

The proposed insulation consists of water trapped in a quilting and therefore quiescent relative to the iceberg. For water of conductivity k and a quiescent layer of water of thickness τ, the equivalent h due to the insulation is simply k/τ. With k = 0.1388 cal/m-sec-°C, an equivalent h of 4.75 can be achieved with a quilting thickness of (0.1388)/4.75 = 0.0292 m or 2.92 cm. With insulation, the loss should be based upon the time-averaged temperature of 15.3°C instead of the distance average temperature of 17.8°C. By adjusting for this factor (15.3/17.8), losses could be held to 10 percent or 30 m with 2.5 cm of insulating water. For other insulation thicknesses (τ cm), the corresponding loss will be $75/\tau$ (meters).

Appendix C

THE COST OF MOVING ICEBERGS

The cost of moving icebergs will depend on the speed. There are two cost factors that are normally influenced by speed in opposite ways. The fuel costs will usually increase with speed, while capital and many operational costs are usually time charges that tend to decrease with increasing speed or less transit time. If there is no constraint on the scheduling so that the equipment can be kept gainfully employed independent of the speed, then there would be some optimum speed at which the ice would be delivered at minimum cost per unit. The simple movement of iceberg trains from Antarctica will most likely require the acquisition of icebergs and ice-train formation in the daylight sea-ice thawing season, and efficient operations could most easily be designed around a 1- or 2-year cycle. The cost of moving the asymptotic ice train discussed in this report on a 1-year cycle will first be estimated, and then the possible improvement in cost at optimum speed will be explored.

The transport operation will assume shrouded propellers driven by electric motors strapped to the sides of the iceberg train, as suggested by the conceptual illustration in the Summary. The power could be provided from a fossil fuel power plant on an escort ship at less development and capital costs than the system that will be estimated here. However, the potential advantages of nuclear power suggest that it is the appropriate ultimate power supply. The potential magnitude of the eventual transport operations and costs so dominate any expected development costs that the latter have been neglected in estimating the

total operational costs. This is *not* to say that the development costs will be small or easy to acquire, but rather that the total costs will eventually be determined principally by the operational costs.

Cost estimates of future systems and comparisons with past systems are difficult when the time spanned involves large changes in monetary values. However, the rough costing needed for feasibility evaluation at this time should be satisfied with future estimates based on 1972 dollars. The estimated costs are for a Light Water Reactor (LWR) power plant with a capacity of 10^6 kW(e) adapted from the designs of floating power plants by Offshore Power Systems. Additional power-plant costing background was obtained from Refs. 33-36. The shipping costs are extrapolated from Refs. 36-38. Other costs were obtained from supplier's esmates. The capital investment required would include:

Floating, seaworthy, LWR power plant, 10^6 kW(e)	$\$350 \times 10^6$
Power distribution, electric motors and propeller systems	40×10^6
Four auxiliary ships (icebreakers, supply, and general purpose)	54×10^6
	$\$444 \times 10^6$

The annual revenue requirements to recover all costs are then estimated as follows:

Amortization of capital investment at a 30-year annual rate of 1/12 of initial investment	$\$37 \times 10^6$
Insurance at 1.5 percent of investment	7×10^6
Power plant fuel	12×10^6
Operation and maintenance of power plant, including nuclear liability insurance	4×10^6
100-man crew other than for power plant	4×10^6
Insulation (∿5000 tons)	15×10^6
Wire rope harness (∿6000 tons)	5×10^6
Special iceberg preparation equipment	1×10^6
Annual cost for acquiring 1.22×10^{13} kg (10^7 acre-ft)	$\$85 \times 10^6$
Cost for 90 percent delivery factor	∿$\$7.7/k\cdot m^3$ (∿\$9.5/acre-ft)

An approximate analytical representation of the total costs, C_T, is the following:

$$C_T = \frac{C_1}{V} + C_2 V^{\beta\eta-1} + C_3 V^{\eta} + C_4 \ , \qquad \text{(C-1)}$$

where $\frac{C_1}{V}$ = costs proportional to time and independent of power, and therefore approximately proportional to 1/V where V is the towing velocity,

$\simeq \$13 \times 10^6$ in the above 1-year cycle illustration,

$C_2 V^{\beta\eta-1}$ = capital costs proportional to time and also dependent on power, i.e., cost $\propto P^{\beta}$ and power, $P \propto V^{\eta}$, and the time dependence represented by 1/V,

$\simeq \$39 \times 10^6$ in the above 1-year cycle illustration,

$C_3 V^{\eta}$ = fuel costs = $\$12 \times 10^6$ in the illustration,

C_4 = costs independent of time, power, or V,

$= \$21 \times 10^6$ in the illustration,

$\beta \simeq 0.7$ for the above power plant and equipment,

η = between 1 and 2 for iceberg trains.

For conventional shipping $\eta \to 2.0$, but for asymptotic iceberg trains at very slow speeds, Coriolis resistances will dominate at high latitudes and $\eta \to 1.0$.

The minimum value of C_T with respect to V is obtained for

$$C_3 V^{\eta} = \frac{1}{\eta} \frac{C_1}{V} + \left(\frac{1 - 0.7\eta}{\eta} \right) C_2 V^{0.7\eta-1} \ . \qquad \text{(C-2)}$$

For $\eta \to 1.0$

$$C_3 V \simeq \frac{C_1}{V} + 0.3 C_2 V^{-0.3} \ ,$$

or the fuel costs are greater than the C_1/V costs.

For $\eta \simeq 1/0.7$

$$C_3 V^{1.4} = 0.7 \frac{C_1}{V} ,$$

or the fuel costs are 0.7 of the C_1/V costs.

For $\eta \to 2.0$

$$C_3 V^2 = \frac{1}{2} \frac{C_1}{V} - 0.2 C_2 V^{0.4} ,$$

or the fuel costs are less than half the C_1/V costs.

The estimated costs for the asymptotic 1-year cycle illustration show fuel costs at about 0.9 of the C_1/V costs, which are within the accuracy range of the approximations for optimum V, so little cost improvement is expected for more nearly optimum speed. The asymptotic 1-year cycle illustration involves variation in V and η. Near the Antarctic, Coriolis forces will dominate, $\eta \to 1.0$, and V will be the smallest. Near the equator, Coriolis forces are negligible, $\eta \to 2.0$, and V will have its largest value. Thus the analytic determination of minimum C_T as indicated in Eq. (C-2) must be a very crude approximation. In order to obtain better results it would probably be necessary to model the transit with small changes in propelling force (or power) about the asymptotic case value of 10^8 N.

Appendix D

ICEBERG TRANSPORT AND MODELS

INTRODUCTION

The transport calculations and modeling are required to determine the relations between iceberg dimensions, propelling force and trip time over selected routes, all as a function of the many parameters that are involved. As was discussed in the body of the report, there are strong economic arguments for operating on a 1-year (or possibly 2-year) cycle that would keep the equipment and personnel gainfully occupied and permit iceberg acquisition in the Antarctic daylight thawing season from December through March.

Two routes representative of quite different ocean environments between the Ross Sea and Los Angeles were selected and illustrated in Fig. 3. The currents and winds encountered along any route are dependent upon the calendar date. Each route is subdivided into 5° intervals of latitude. Environmental conditions representative of the midpoints of these intervals were taken from Refs. 22 and 39-42; the transit time was calculated for each 5° interval. Average drift currents were used and the transit speed was computed for each of (usually) eight wind directions where wind force and frequency were taken from the wind roses of pilot charts. The weighted average speed is the sum of transit speeds corresponding to each wind direction weighted by the fraction of the time that wind direction (and transit speed) would be expected. Numerical data describing the routes are given in Table D-1 (long route) and Table D-2 (short route). The third column of each table gives the month for which the current and wind data were taken,

Table D-1

NUMERICAL DATA FOR LONG ROUTE

LAT	LON	MONTH	TRANSIT DIST	MOTION COURSE	--CURRENT-- SPEED	DIR	--------WIND, FORCE AND PERCENT OF TIME-------- --N-	-NE-	--E-	-SE-	--S-	-SW-	--W-	-NW-
-70.	-170.	MAR	1089.	77.	0.33	72.	1 0	1 0	1 0	1 0	1 0	4 1	4 98	4 1
-65.	-123.	APR	579.	56.	0.33	63.	1 0	1 0	1 0	1 0	1 0	5 1	5 98	5 1
-60.	-105.	JUN	463.	52.	0.04	49.	5 14	5 14	5 11	4 4	6 13	6 11	6 18	6 15
-55.	-94.	JUN	394.	38.	0.10	46.	5 9	4 7	5 8	5 12	5 13	6 15	6 21	6 15
-50.	-87.	JLY	362.	33.	0.30	358.	4 12	6 5	4 10	5 15	5 15	6 15	4 18	4 10
-45.	-82.	AUG	328.	26.	0.08	325.	5 9	4 4	4 5	5 8	4 13	6 19	5 24	5 18
-40.	-79.	AUG	315.	17.	0.41	335.	3 10	5 4	5 4	4 11	4 20	5 12	4 17	6 20
-35.	-77.	SEP	304.	7.	0.28	26.	4 11	4 8	3 6	4 15	4 20	4 17	3 11	4 12
-30.	-76.	SEP	305.	359.	0.20	300.	2 4	1 4	4 4	4 41	4 32	4 7	3 4	2 4
-25.	-77.	SEP	305.	348.	0.41	290.	2 2	2 2	4 8	4 61	3 22	2 1	1 2	2 2
-20.	-78.	SEP	321.	338.	0.60	289.	2 2	3 2	3 29	5 63	2 1	1 0	4 1	3 2
-15.	-80.	OCT	419.	320.	1.17	298.	1 0	3 2	3 10	4 75	3 8	3 3	1 0	3 2
-10.	-85.	OCT	422.	311.	0.33	321.	2 2	2 2	4 9	3 69	4 12	2 4	3 2	1 0
-5.	-90.	OCT	670.	297.	0.56	270.	2 2	3 1	3 10	3 60	2 21	3 2	3 2	2 2
0.	-100.	NOV	463.	297.	0.84	286.	1 0	5 2	3 6	3 48	4 41	3 2	1 1	1 0
5.	-106.	NOV	422.	0.	0.22	81.	2 7	3 12	3 4	3 16	3 45	4 10	3 2	2 4
10.	-111.	DEC	348.	327.	0.29	300.	4 6	4 57	3 26	4 6	4 3	3 1	1 0	1 1
15.	-114.	DEC	346.	327.	0.48	277.	3 18	4 34	3 16	4 5	3 4	3 3	3 4	3 16
20.	-117.	DEC	300.	353.	0.19	245.	3 27	4 31	4 8	3 3	3 4	3 3	3 6	3 18
25.	-117.	DEC	300.	353.	0.05	262.	4 31	4 7	3 5	4 4	3 4	3 4	3 6	4 39
30.	-117.	JAN	200.	353.	0.02	250.	4 31	4 6	3 5	4 4	3 4	3 5	3 6	4 39
33.	-118.													

Table D-2

NUMERICAL DATA FOR SHORT ROUTE

LAT	LON	MONTH	TRANSIT DIST	MOTION COURSE	--CURRENT-- SPEED	DIR	--N-	-NE-	--E-	-SE-	--S-	-SW-	--W-	-NW-
							-------WIND, FORCE AND PERCENT OF TIME--------							
-70.	-170.	MAR	490.	53.	0.33	72.	1 0	1 0	1 0	1 0	1 0	4 1	4 98	4 1
-65.	-153.	APR	407.	44.	0.33	63.	1 0	1 0	1 0	1 0	1 0	5 1	5 98	5 1
-60.	-143.	APR	357.	35.	0.0	0.	5 16	4 8	3 9	4 7	5 7	6 17	5 19	6 17
-55.	-137.	MAY	351.	29.	0.14	94.	5 20	4 2	3 5	3 5	4 5	7 22	5 30	6 11
-50.	-132.	JUN	341.	27.	0.0	0.	6 11	5 8	4 14	4 11	5 10	6 18	5 20	6 9
-45.	-128.	JUN	328.	26.	0.0	0.	7 2	5 15	5 13	5 8	5 6	6 12	4 22	4 22
-40.	-125.	JLY	332.	25.	0.0	0.	5 10	4 7	4 10	4 11	5 10	5 18	6 19	4 15
-35.	-122.	AUG	317.	19.	0.11	127.	4 10	5 10	4 11	4 10	5 13	5 14	5 17	4 15
-30.	-120.	AUG	318.	18.	0.06	303.	4 16	4 12	4 13	4 16	4 12	4 11	3 7	4 13
-25.	-118.	AUG	305.	11.	0.05	306.	4 9	4 14	4 31	4 21	3 11	3 4	4 5	5 5
-20.	-117.	SEP	305.	11.	0.13	254.	3 8	3 14	4 52	4 13	5 4	2 3	3 3	3 3
-15.	-116.	SEP	306.	11.	0.18	255.	3 1	4 12	4 66	4 19	2 1	1 0	1 0	2 1
-10.	-115.	SEP	306.	11.	0.40	270.	1 0	4 6	4 61	4 30	2 1	2 1	2 1	1 0
-5.	-114.	OCT	306.	11.	0.58	254.	1 1	4 6	4 48	3 40	4 2	2 1	1 0	3 2
0.	-113.	OCT	306.	11.	1.07	290.	1 0	5 2	3 6	4 57	4 30	3 4	1 0	2 1
5.	-112.	OCT	306.	11.	0.07	229.	1 1	1 0	3 3	3 14	4 68	3 12	2 2	1 0
10.	-111.	NOV	343.	327.	0.14	323.	3 13	4 41	4 27	3 7	3 5	4 4	1 0	1 3
15.	-114.	NOV	346.	327.	0.32	276.	3 27	4 19	4 11	3 5	3 2	3 4	2 6	3 26
20.	-117.	NOV	300.	358.	0.21	188.	3 26	4 30	4 10	3 2	2 2	3 2	3 6	3 22
25.	-117.	NOV	300.	358.	0.23	205.	2 32	3 5	3 2	2 2	2 3	2 3	3 8	4 45
30.	-117.	DEC	200.	358.	0.05	6.	2 16	3 8	3 7	3 6	2 8	2 9	3 12	3 34
33.	-118.													

based upon a "base case" transit configuration. The distance (in n mi) is the length of each leg; directions are measured clockwise from north; current speed is in knots; the direction is the average direction of the drift. The wind in each octant is described by two numbers. The first number is the Beaufort force; the second is the percentage of the time that the wind blows from the indicated direction (N, NE, etc.).

It is clear that the transport calculations are based upon a prechosen route and a corresponding sequence of current and wind conditions. As the iceberg size and shape are varied, the propelling force is also varied so that the total trip time is approximately 10 months. The actual trip time in some cases deviates by as much as two months from the nominal trip time so that the calendar dates are not strictly satisfied by the transit times. This calendar slippage is not regarded as a particularly significant factor in the overall calculation; other and much greater uncertainties appear in much of the data.

Ocean currents, described by magnitude and direction, have been observed at a small number of sampling stations. For iceberg transport, it would be desirable to have an extensive survey of the currents (down to a depth of 250 m) along proposed routes. Such data do not exist, and the calculations performed here are based upon the assumption that the surface drift currents extend to a depth of 250 m on both of the two chosen routes. The currents are helpful in reducing total transit time compared to traversing the same route in the absence of currents.

For large icebergs at latitudes greater than 20° or so, Coriolis effects may be quite pronounced. There is uncertainty over the effect of the water displaced by the iceberg and the fact that its net motion is in the opposite direction to that of the iceberg. The deflection of this water by the Coriolis force should produce an interaction of the water and the iceberg so as to partially cancel the effects of the direct force acting on the iceberg, as has been discussed in the body of this report and in Appendix E.

MODELING THE CORIOLIS AND DRAG FORCES

A relatively simple model of the transport problem can be con-

structed if winds and currents are neglected. The configuration is illustrated in Fig. D-1. The iceberg, of length ℓ and width ω, is moved with speed V by a force of magnitude T. The figure, applicable in the Southern Hemisphere, shows the propelling force at angle β to the velocity vector and a Coriolis force F_c, acting at right angles to the velocity vector. This propelling force will hereafter be referred to as a thrust, whether conceived as a tow-line tension or derived from side-mounted propellers.

The figure illustrates the fact that a component of the thrust vector may be used to offset the Coriolis force. The figure is otherwise incomplete. In order to derive an equilibrium speed, it is necessary to introduce drag forces.

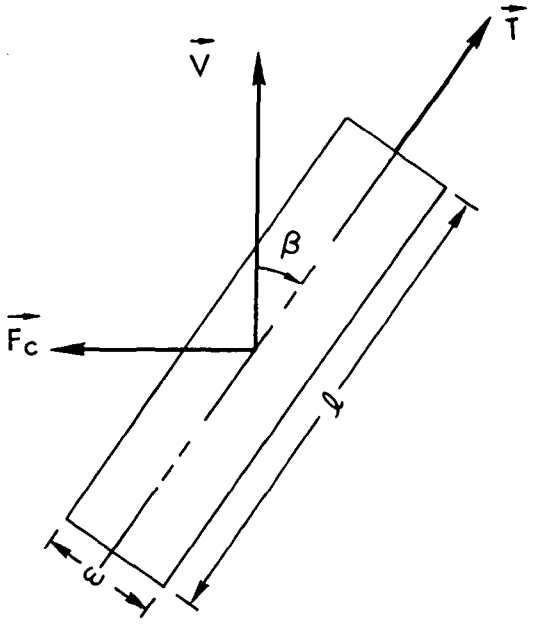

Fig. D-1 — Basic Transport Configuration

Figure D-2 illustrates the force components as resolved parallel and perpendicular to the thrust vector. The Coriolis force components are

$$F_c \text{ (parallel)} = 2mV\Omega \sin \varphi \sin \beta \,, \qquad \text{(D-1a)}$$

$$F_c \text{ (normal)} = 2mV\Omega \sin \varphi \cos \beta \,, \qquad \text{(D-1b)}$$

where m = mass,

Ω = earth's rotation (7.29×10^{-5} rad/sec),

φ = latitude (negative in the Southern Hemisphere),

V = speed,

β = thrust angle.

A parallel force component is positive if it acts with the thrust vector (+y direction); a normal force is positive if it acts in the +x direction. With these conventions, β will be a positive angle when propelling in the Southern Hemisphere.

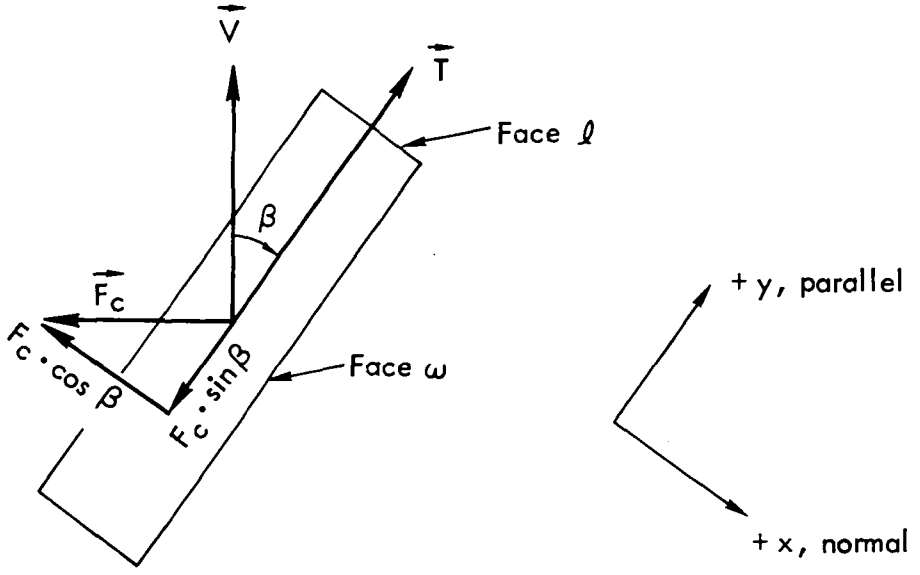

Fig. D-2 — Coriolis Force Components

The quantity [$\Omega \sin \varphi$] is sometimes termed the Coriolis parameter. In the present work, a quantity J is defined by

$$J = k\Omega \sin \varphi \, . \tag{D-2}$$

The symbol k, termed the Coriolis fraction, is used to represent the fraction of the total Coriolis force that is effective in deflecting the iceberg. The water displaced by the forward-moving iceberg must flow around and under the iceberg. That mass of rearward-flowing displaced water is also subject to the Coriolis force, but in a direction opposite to the direct force on the iceberg. It may be interpreted that the water on one side of the iceberg is deflected toward the iceberg; on the other side it is deflected away; and a difference in water level on the two sides provides a mechanism for the appearance of a force opposing the direct Coriolis force on the iceberg. For the parameters used in this study, a static head difference of less than one centimeter of water would suffice to totally offset the Coriolis force.

The Coriolis force can be a dominant factor in iceberg movement, and the appropriate value of k is highly uncertain. A very crude argument attributes the water counterforce to that portion of the water that flows by the sides, but not under the iceberg. As was discussed in the body of the report, it should be possible to select the icebergs and design the transport operations so that k will be 0.5 or less. A resolution of the apparent conflict between the concept of a rearward-moving mass of displaced water and a common concept of virtual mass is described in Appendix E.

There are two kinds of drag forces: forces normal to the faces (dynamic pressure forces) and forces tangential to the faces (skin friction). The normal and tangential surface forces are given by

$F_{\parallel}$ = the normal force acting on the frontal area and therefore parallel to the long axis of the iceberg;

$$= -\tfrac{1}{2} C_{\ell} A'_{\ell} \rho' V^2 \, |\cos \beta| \cdot \cos \beta \, . \tag{D-3}$$

$F_{\perp}$ = the normal force acting on the side area and therefore perpendicular to the long axis of the iceberg;

$$= \tfrac{1}{2} C_{\omega} A'_{\omega} \rho' V^2 \, |\sin \beta| \cdot \sin \beta \, . \qquad \text{(D-4)}$$

$F'_{\perp}$ = the tangential force acting on the frontal area and therefore perpendicular to the long axis of the iceberg;

$$= \text{neglected} \, .$$

$F'_{\parallel}$ = the tangential force acting on the side area and therefore parallel to the long axis of the iceberg;

$$= -\tfrac{1}{2} f_{\omega} A'_{\omega} \rho' V^2 \, |\cos \beta| \cdot \cos \beta \, . \qquad \text{(D-5)}$$

$F'_{B,\parallel}$ = that component of the tangential force on the bottom, which acts parallel to the long axis of the iceberg;

$$= -\tfrac{1}{2} f_0 A'_h \rho' V^2 \cos \beta \, . \qquad \text{(D-6)}$$

$F'_{B,\perp}$ = the component of the tangential force on the bottom, which acts perpendicular to the long axis of the iceberg;

$$= \tfrac{1}{2} f_0 A'_h \rho' V^2 \sin \beta \, . \qquad \text{(D-7)}$$

The face areas are subscripted by the dimensions (ℓ,ω,h) to which they are orthogonal. The other quantities are: C_{ℓ} = the ratio of force per unit area (on the frontal area) to dynamic pressure $\frac{1}{2}\rho V^2$; C_{ω} = the ratio of force per unit area (on the side area) to dynamic pressure $\frac{1}{2}\rho V^2$; f_{ω} = the friction coefficient for the side area based upon a Reynolds number defined by the iceberg length and characteristic speed V cos β; f_0 = the friction coefficient for the bottom area based upon a Reynolds number defined by an average path length for the orientation β with the full relative speed V. The seawater density is ρ'.

The normal force equations, Eqs. (D-3) and (D-4), can be viewed as derived from relative velocity components $V \cdot \cos \beta$ on the front face and $V \cdot \sin \beta$ on the side face. These derive from a flat-plate dynamic drag picture where the side-face coefficient, $C_\omega \simeq 1$, represents a vertical flat-plate effect; the front-face coefficient, C_ℓ, with values ranging from 0.1 to 0.6, is intended to represent varying degrees of bow rounding that might be achieved by permissive ablation. These coefficients are treated as independent of β; the entirety of the attitude-dependent characteristics are absorbed in the relative velocity components. This apparently heavy-handed interpolation process seems to be the only simple way of handling a situation in which β can range from nearly $-\pi$ to nearly $+\pi$ under various conditions of currents and winds.

The vertical areas A'_ℓ and A'_ω are submerged areas and are related to the total area of those faces by

$$\rho' A'_\ell = \rho A_\ell = \rho \cdot \frac{\ell \omega h}{\ell} = \frac{m}{\ell} , \tag{D-8}$$

$$\rho' A'_\omega = \rho A_\omega = \rho \cdot \frac{\ell \omega h}{\omega} = \frac{m}{\omega} , \tag{D-9}$$

where ρ = the density of ice, and $m(= \rho \cdot \ell \omega h)$ = the iceberg mass. The bottom area is similarly represented by taking the density of ice as 5/6 that of water and

$$\rho' A'_h = \frac{5}{6} \cdot \frac{m}{h} . \tag{D-10}$$

With the preceding equations for drag forces, the parallel and normal forces can be summed to the following:

Summation of the forces acting parallel to the long axis

$$= -\left[\left(\frac{C_\ell}{\ell} + \frac{2 f_\omega}{\omega} \right) |\cos \beta| + \frac{5}{6} \frac{f_0}{h} \right] \cdot \tfrac{1}{2} m V^2 \cos \beta . \tag{D-11}$$

Summation of the perpendicularly acting hydrodynamic forces

$$= \left[\frac{C_\omega}{\omega} \left| \sin \beta \right| + \frac{5}{6} \frac{f_0}{h} \right] \cdot \tfrac{1}{2} m V^2 \sin \beta \ . \qquad \text{(D-12)}$$

These force components are combined with the Coriolis components to provide thrust equations valid in the absence of current and wind:

$$2JV \sin \beta - \frac{1}{2L} V^2 \cos \beta = -T/m. \qquad \text{(D-13)}$$

$$2JV \cos \beta + \frac{1}{2W} V^2 \sin \beta = 0 \ . \qquad \text{(D-14)}$$

$$J = k\Omega \sin \varphi \ ,$$

$$\frac{1}{L} = \left(\frac{C_\ell}{\ell} + \frac{2f_\omega}{\omega} \right) \left| \cos \beta \right| + \frac{5}{6} \frac{f_0}{h} \ , \qquad \text{(D-15)}$$

$$\frac{1}{W} = \frac{C_\omega}{\omega} \left| \sin \beta \right| + \frac{5}{6} \frac{f_0}{h} \ .$$

The quantities L and W have dimensions of length and summarize combinations of several parameters.

EFFECTS OF OCEAN CURRENTS

If an iceberg drifts freely in a current, then it may be assumed that it partakes of the same motion as does the water it displaces. No forces appear or are required unless the iceberg is moved relative to the current. Thus all of the preceding calculations are valid if referred to a coordinate system moving with the current.

A minor complication arises when a specific geographic course-made-good is prescribed. Up to this point, geographical coordinates have been unnecessary; the magnitude of the Coriolis force depends upon the magnitude, but not the direction, of the velocity vector. The additional prescription of a course to be made good in the presence of a

current provides an additional constraint as illustrated in Fig. D-3. At any latitude, it is possible to calculate the speed V that can be made relative to the current. If U is the speed-made-good (geographically), then U satisfies the equation

$$V^2 = U^2 + V_c^2 - 2UV_c \cos(\gamma - \alpha) .$$

The solution for U is

$$U = V_c \cos(\gamma - \alpha) \pm \sqrt{V^2 - V_c^2 \sin^2(\gamma - \alpha)} . \qquad \text{(D-16)}$$

Choice of the positive sign provides the largest possible positive speed, but real solutions do not necessarily exist (e.g., the speed may be insufficient to counter the current). In awkward cases it may be necessary to reroute by choosing a new course α in order to find a real, positive speed U.

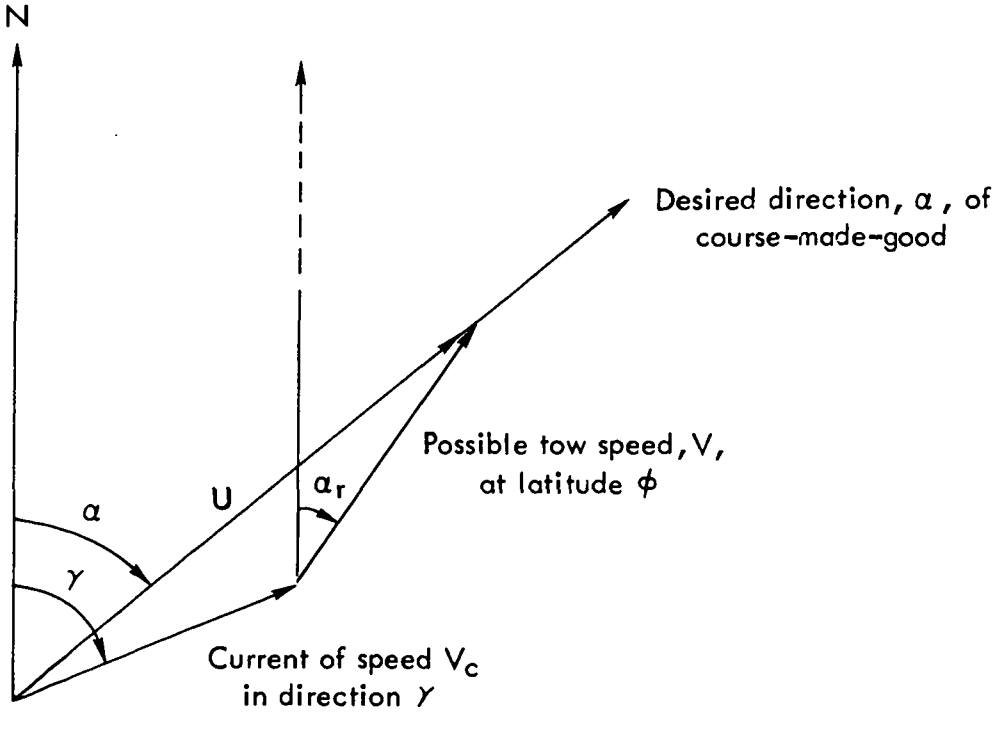

Fig. D-3 — Effect of currents

In solving the above problem, the angle β is the angle between the direction of thrust and the direction of the velocity vector $\vec{V}$. The thrust angle relative to north ($\beta_0 = \beta + \alpha_r$) represents the geographically referenced orientation of the iceberg. To effect this transformation, the angle α_r is given by

$$\alpha_r = \tan^{-1}\left(\frac{U \sin \alpha - V_c \sin \gamma}{U \cos \alpha - V_c \cos \gamma}\right). \qquad \text{(D-17)}$$

EFFECTS OF WIND

The dynamic pressures due to the wind are similar to those due to water drag. Equations (D-3) and (D-4) will be valid if the angle β is replaced with the angle η representing the wind direction relative to the thrust vector (Fig. D-4), and by using freeboard areas in place of submerged areas. The direction from which the wind is coming is ψ; the relative wind direction is $\eta = \beta_0 - \psi$; and no correction is made for the small velocity of the iceberg.

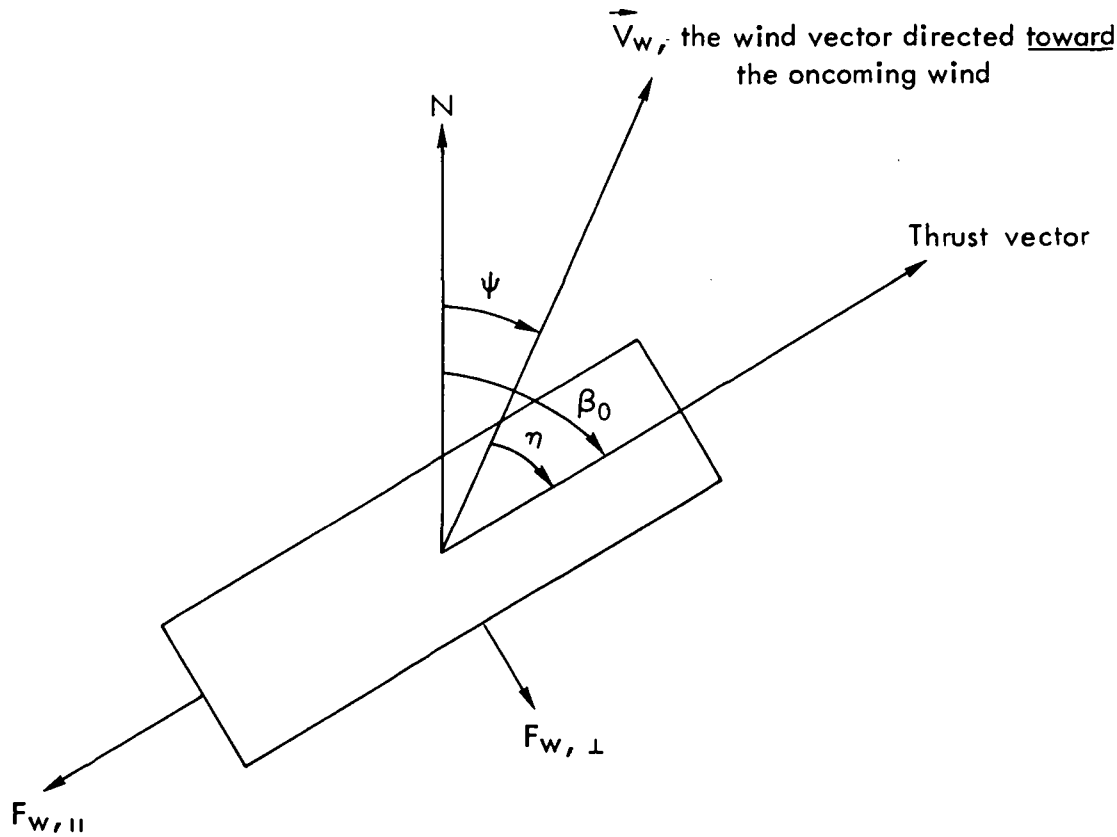

Fig. D-4 — Wind effects

By analogy with Eqs. (D-3) and (D-4), the parallel and perpendicular force components due to the wind are

$$F_{W,\parallel} = -\frac{1}{12}\rho_a V_w^2 C_\ell h\omega \cdot |\cos\eta| \cdot \cos\eta \ . \qquad \text{(D-18)}$$

$$F_{W,\perp} = \frac{1}{12}\rho_a V_w^2 C_\omega h\ell \cdot |\sin\eta| \cdot \sin\eta \ . \qquad \text{(D-19)}$$

A factor of 6 has been introduced to reduce the total height h to the freeboard height, h/6. The wind speed and density are V_w and ρ_a, respectively.

THE COMPLETE MODEL

The equations describing the transport are Eqs. (D-13) and (D-14) as augmented by the wind forces of Eqs. (D-18) and (D-19) and the transformation from the coordinate system moving with the current to the geographical coordinate system. The equations for the force balances are

$$2JV \sin\beta \cdot \frac{1}{2L} V^2 \cos\beta = -T/m + \tfrac{1}{2}\rho_a V_w^2 C_\ell h\omega \, |\cos\eta| \cdot \cos\eta \ . \qquad \text{(D-20)}$$

$$2JV \cos\beta + \frac{1}{2W} V^2 \sin\beta = -\tfrac{1}{2}\rho_a V_w^2 C_\omega h\ell \, |\sin\eta| \cdot \sin\eta \ . \qquad \text{(D-21)}$$

The definitions of J, L, and W are given by Eq. (D-15).

The necessary coordinate transformations are given by Eqs. (D-16) and (D-17):

$$U = V_c \cos(\gamma - \alpha) + \sqrt{V^2 - V_c^2 \sin^2(\gamma - \alpha)} \ ,$$

$$\alpha_r = \tan^{-1}\left(\frac{U \sin\alpha - V_c \sin\gamma}{U \cos\alpha - V_c \sin\gamma}\right) .$$

The relative wind direction η is related to the true wind direction ψ, the thrust angle β, and the direction of the iceberg velocity

vector relative to the current, α_r, according to

$$\eta = \beta - \alpha_r - \psi \ . \qquad \text{(D-22)}$$

Equations (D-16), (D-17), (D-20), (D-21), and (D-22) have been solved by a (usually) convergent iterative procedure. Various iceberg sizes and shapes under various propelling forces have been treated under typical conditions of wind and current along the routes indicated in Fig. 3. The results of these computations are described in the following paragraphs.

RESULTS AND PARAMETER SENSITIVITIES

Figure D-5 illustrates transport results on the long, coastal route for an iceberg train 80 km long, 600 m wide, and 300 m thick. The thrust of 10^8 N would require approximately 1.35×10^6 horsepower if 16 propellers, which are 36 ft in diameter, are used (see Fig. D-15). The transit time per 5° latitude interval is plotted versus the latitude. The total transit time from 70°S, 170°W to 33.3°N, 118°W is shown in a summary table on the figure. The various dashed curves represent alternative assumptions regarding winds and currents; one or the other or both are suppressed, and are intended to illustrate the relative aid or hindrance of these environmental factors. The number of miles per 5° interval is not uniform because of varying course, but these mileage distances are given along an upper abscissa scale. The currents and winds both have an average beneficial effect along this route; the effect of the current is more pronounced than that of the wind. The Coriolis fraction, k, was set at 1/2 maximum (1/2 of the full theoretical value applied directly to the icebergs) in this computation.

The marked latitude dependence of speeds that can be deduced from Fig. D-5 is indicative of a dominant Coriolis effect upon overall transit time. This is examined in Fig. D-6, which reproduces the computations of Fig. D-5, but with the Coriolis parameter set at zero and the thrust reduced from 10^8 N to 3×10^7 N. The total transit time is somewhat better under these conditions despite the large reduction in thrust. This illustrates the strong dependency of the computation upon the assumptions regarding the Coriolis fraction.

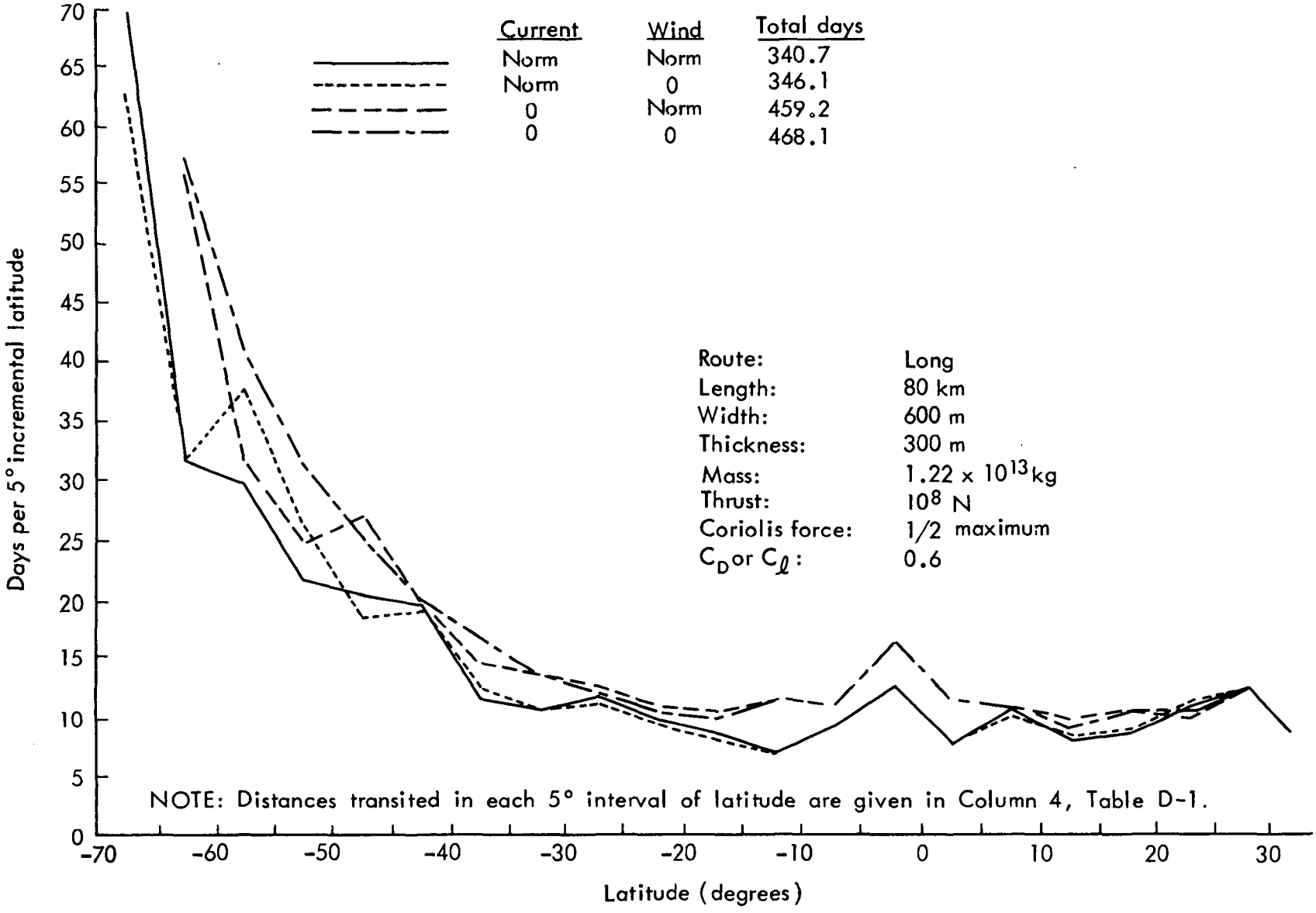

Fig. D-5 — Transit time, long route (k=1/2)

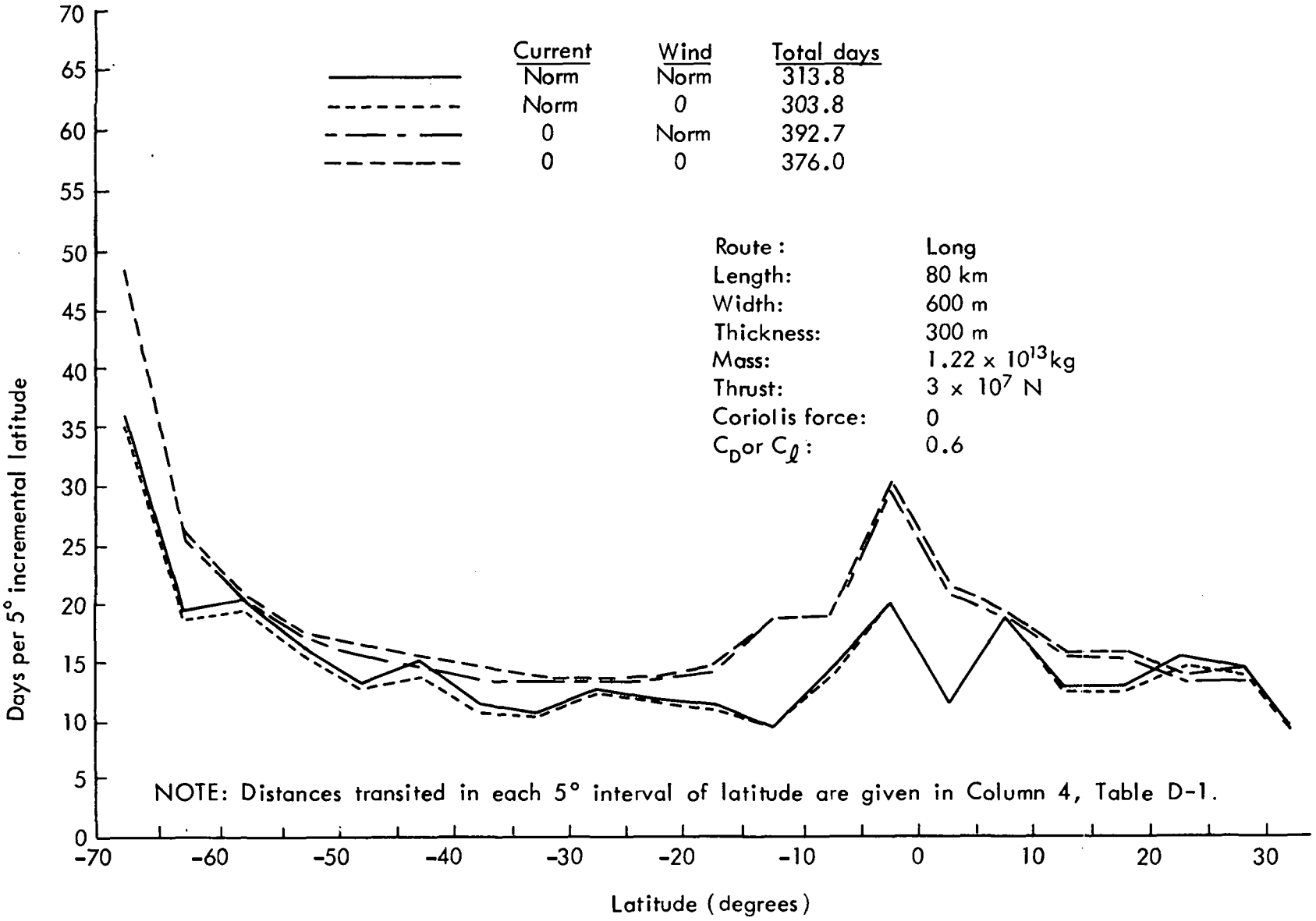

Fig. D-6 — Transit time, long route (k=0)

Figure D-7 shows results for the same configuration propelled along the short (nearly great circle) route with a force of 10^8 N and a Coriolis force of 1/2 the maximum theoretical value. The total transit time along this route is about 85 percent of that required for the long route (Fig. D-5). The winds and currents have less importance relative to the propelling force on this route, but the route is shorter and provides a more rapid departure from the extreme latitude region of large Coriolis forces.

Figure D-8 shows the effect of varying the length/width ratio under constant mass and constant tow force conditions. The behavior near the equator is governed by the form drag (dynamic pressure) and skin friction for which the wider blocks represent better compromises toward minimizing the total drag than do long, narrow blocks. The performance, when more than 20° from the equator, tends to become dominated by the Coriolis force. In these regions the long, thin configuration is superior in generating a "lift" per unit mass, which usefully offsets the Coriolis force.

A comparison of various lengths for fixed width and thickness is given in Fig. D-9. The masses are proportional to volume or length; the thrusts were varied to provide an approximate 10-month transit time. With the very short block (ℓ = 0.8 km), the iterative solution did not converge near the equator with the assumed thrust. The speed possible with this poorly shaped mass of relatively high drag (C_D or C_ℓ = 0.4) did not permit transport on the design path in the region of large equatorial current. In the southern latitudes, it is apparent that the transport resistance of this iceberg is dominated more by drag characteristics than by Coriolis forces. This points up the difficulty of doing small-scale experiments: the drag characteristics are not easily scalable.

Figure D-10 demonstrates the wide fluctuation that can occur under various wind conditions. In all of the preceding figures, the speed-made-good was computed for each of eight wind conditions (direction and force), and the average speed taken as the sum of $f_i V_i$, where f_i is the probability of a wind condition and V_i is the speed-made-good under that wind condition. Figure D-10 shows transit times in each interval for

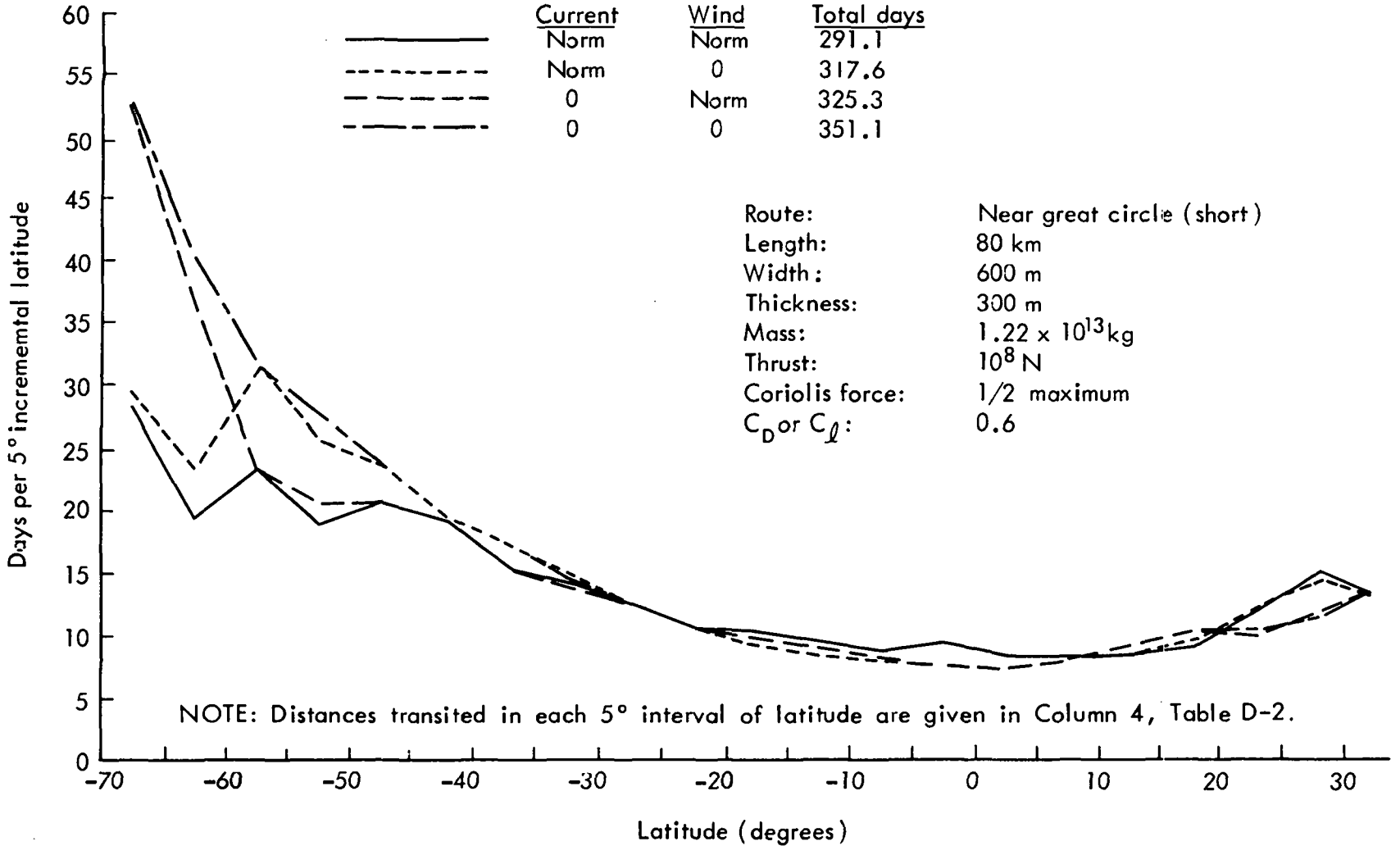

Fig. D-7 — Transit time, short route (k=1/2)

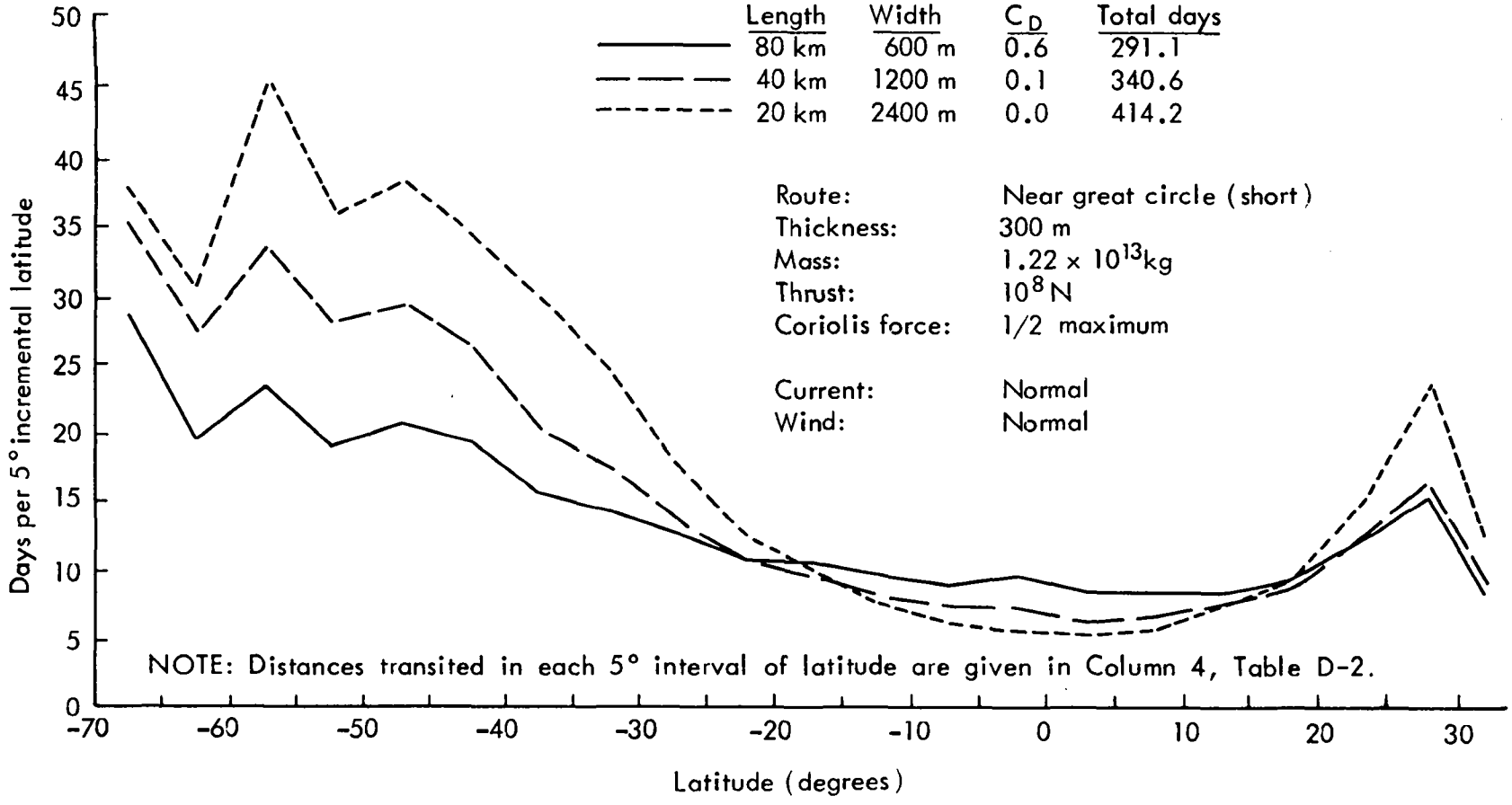

Fig. D-8 — Length/width variations at constant mass

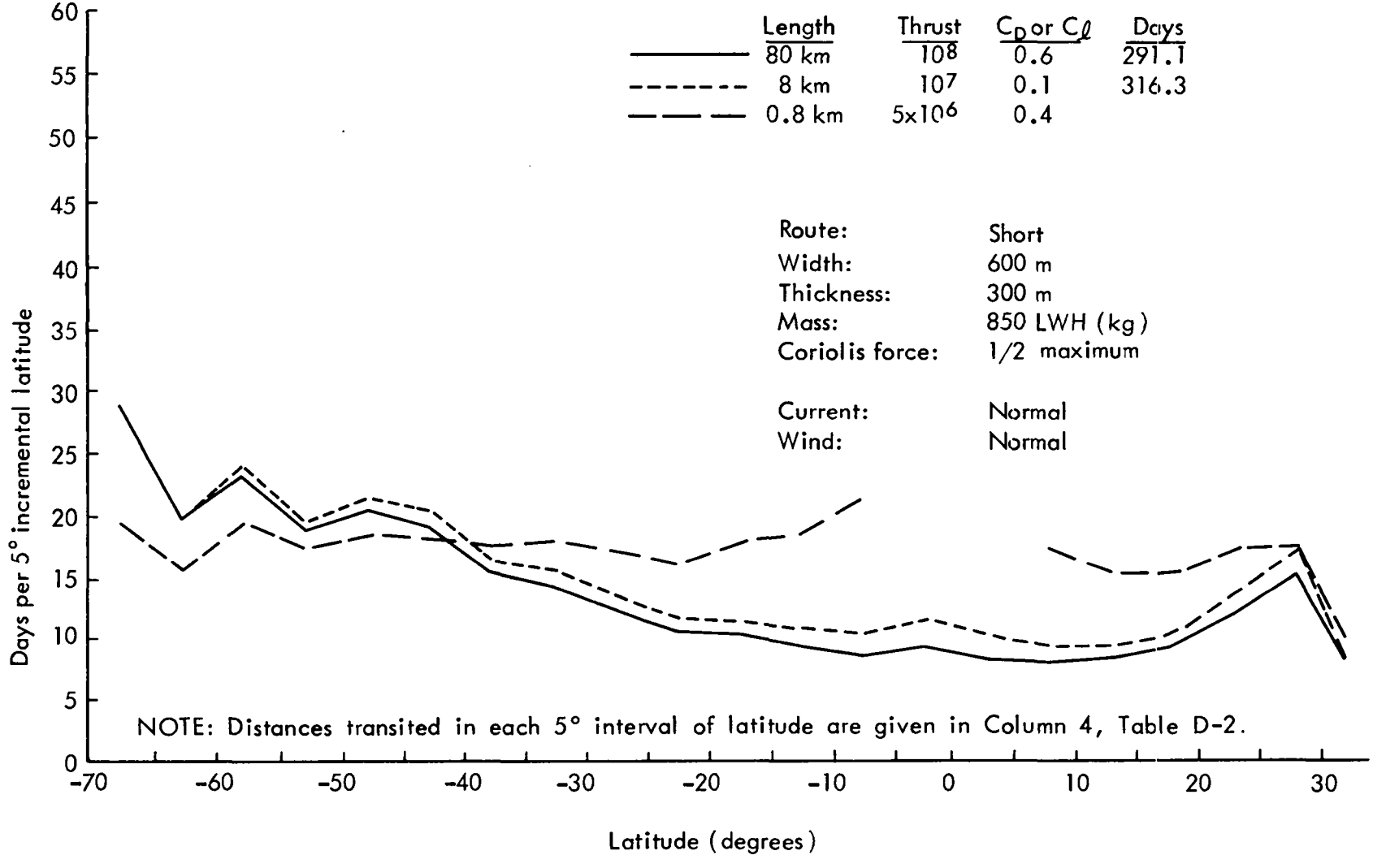

Fig. D-9 — Length variations at constant frontal area

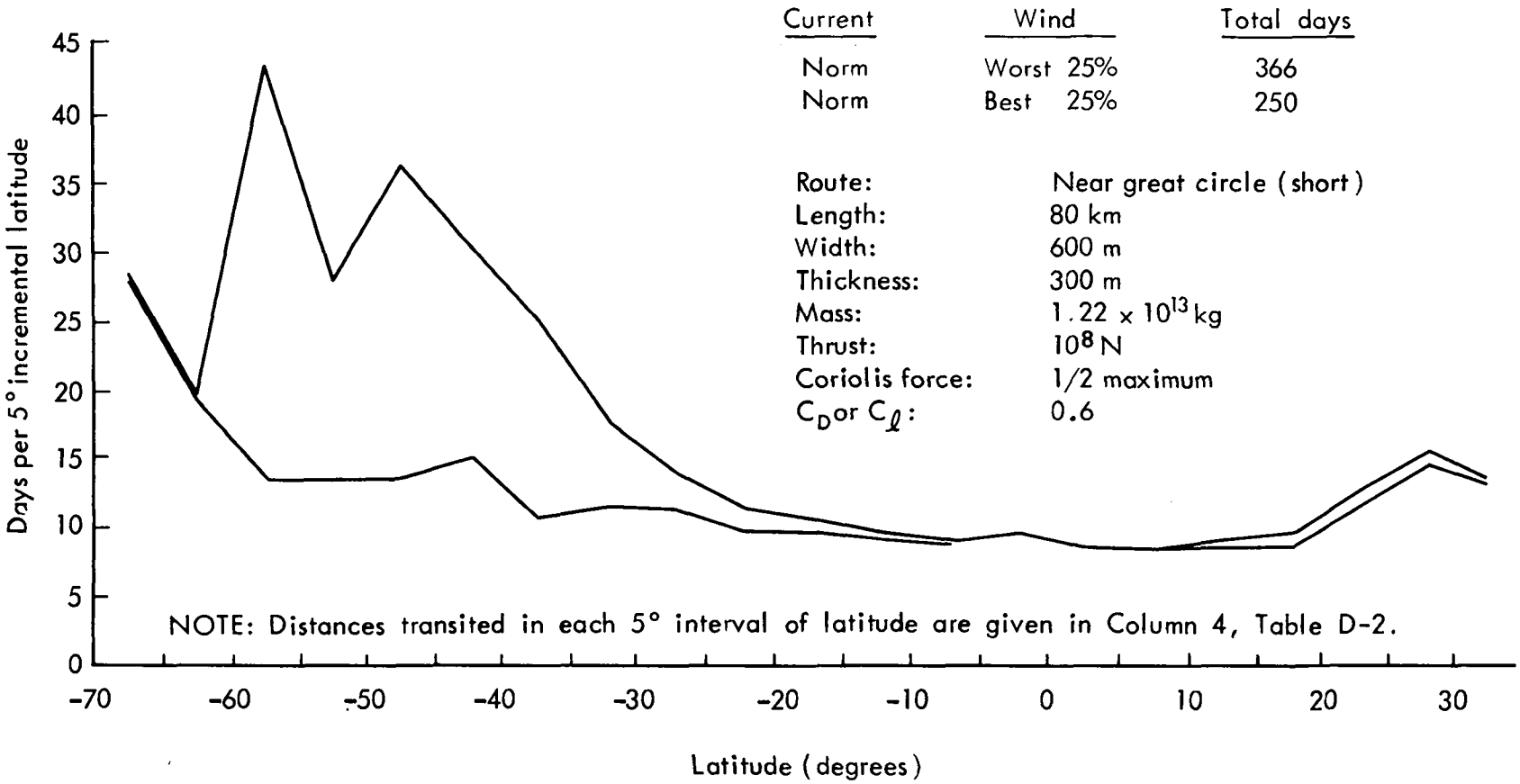

Fig. D-10 — Transit time fluctuations for extreme winds

the best 25 percent of the wind conditions (lower line) and worst 25 percent (upper line). The computation is the one that was used in preparing Fig. D-7 (solid line), and the parameters reported on that figure are valid here. Thus, although the average effect of winds is not very great (see Fig. D-7), the fluctuation in effects is substantial in some regions. The total trip times for these cases range from 250 to 366 days (most favorable 25 percent of the wind conditions to least favorable 25 percent, respectively). A trip exceeding either of these extremes would represent an event of extremely low probability.

AN APPROXIMATE SOLUTION OF TRANSPORT EQUATIONS

The example results presented in the foregoing pages are too specific for some purposes. Computations of that kind will be necessary in the assessment of specific situations (i.e., routes, deliveries, and thrust forces) and should be as realistic as possible. However, there is the problem of estimating the useful ranges of parameters to be examined in a specific situation defined by a desired delivery mass or an available propelling power. To this end, an approximate graphical solution of the equations has been constructed for the zero environmental condition (no wind, no current). The solution gives the speed (and thrust angle β) as a function of latitude, iceberg size and shape, normal force coefficients, and thrust.

The approximate solution is based upon solving simplified versions of Eqs. (D-13), (D-14), and (D-15). These simplified versions are:

$$-2JV \sin \beta + \frac{1}{2L_0} \cdot V^2 \, |\cos \beta| \cdot \cos \beta = T/m \, . \tag{D-23}$$

$$2JV \cos \beta + \frac{1}{2W_0} V^2 \, |\sin \beta| \cdot \sin \beta = 0 \, . \tag{D-24}$$

$$J = k\Omega \sin \varphi \, ,$$

$$\frac{1}{L_0} = \frac{C_\ell}{\ell} + 0.0022 \left(\frac{2}{\omega} + \frac{5}{6h} \right) , \tag{D-25}$$

$$\frac{1}{W_0} = \frac{C_\omega}{\omega} \, .$$

For small icebergs, L_0 is determined largely by C_ℓ/ℓ, and the numeric 0.0022 is not very significant. At the equator, φ and β are both zero so the speed is given by

$$V = \sqrt{2L_0\ T/m}\ . \tag{D-26}$$

The number 0.0022 was chosen in order that V, as computed by Eq. (D-26), would agree well with more exact computations using Reynolds-number-dependent friction factors.

In solving Eq. (D-24) for V,

$$V = -\frac{4JW_0}{|\sin\beta|}\cot\beta\ . \tag{D-27}$$

This can be substituted in Eq. (D-23) to obtain:

$$\frac{\cos\beta}{|\sin\beta|} + \frac{W_0}{L_0}\frac{\cos^3\beta|\cos\beta|}{\sin^4\beta} = \frac{T/m}{8W_0J^2}\ .$$

In the absence of wind and current, $-\pi/2 < \beta < \pi/2$, so that $|\cos\beta| = \cos\beta$. Whether β is positive or negative, the left hand side of this equation will have only positive terms. Consequently it suffices to find the root $0 < \beta < \pi/2$ and note that a corresponding root, $-\beta$, also exists. According to Eq. (D-24), if $J > 0$, then the negative root must be chosen. In most practical transport operations, $|\beta|$ will be less than 45°, and a more convenient form of the transcendental equation is

$$\frac{K}{W_0}\tan^4\beta - \tan^3\beta - \frac{W_0}{L_0} = 0\ , \tag{D-28}$$

$$K = \frac{T/m}{8J^2} = \frac{1}{8J^2}\ (\text{tow force per unit mass})\ .$$

The principal root of Eq. (D-28) is shown in Fig. D-11, which provides a means of calculating the thrust angle β in degrees from the

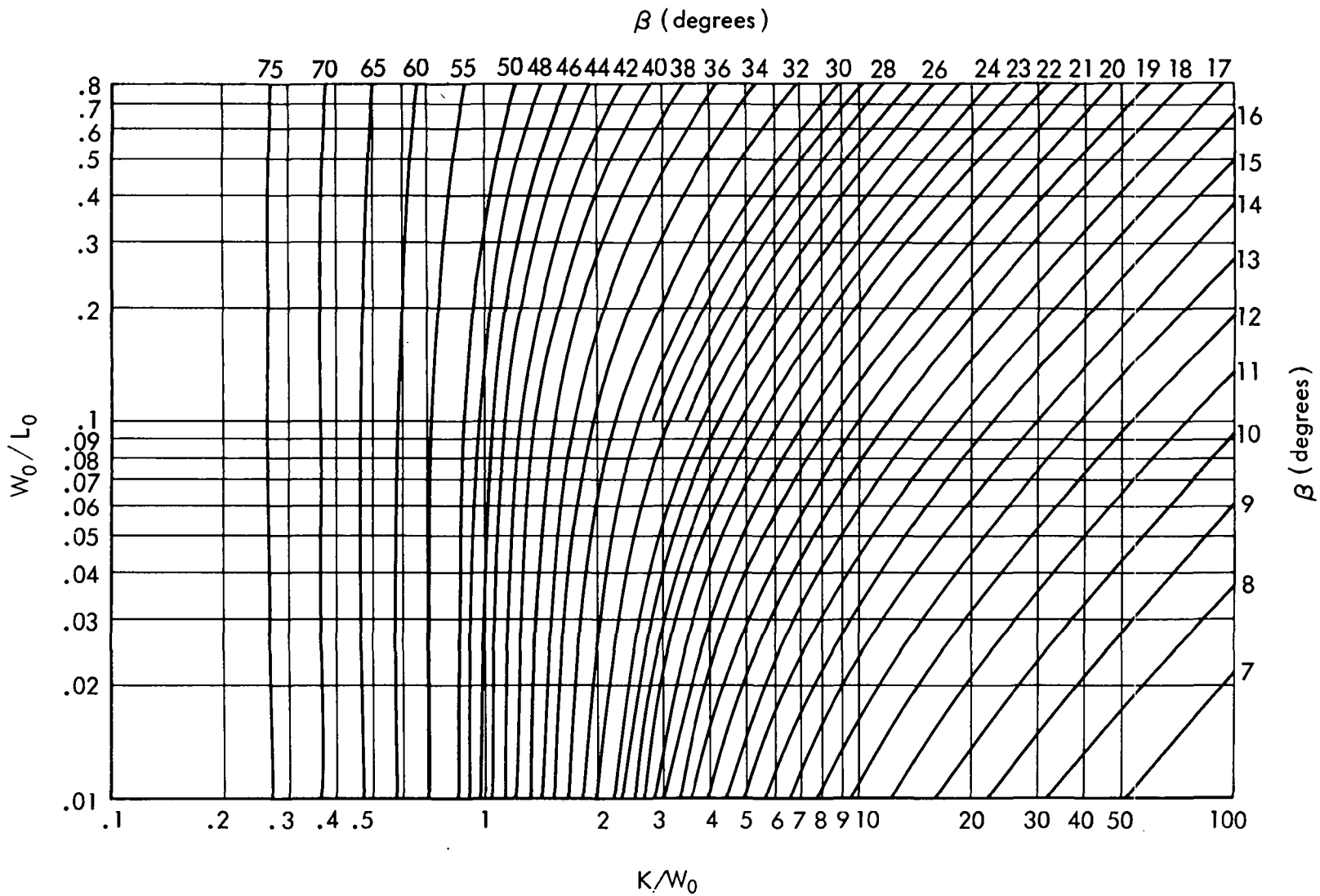

Fig. D-11 — Generalized solution for propelling angle β (degrees)

dimensionless ratios K/W_0 and W_0/L_0. If the length dimensions ℓ and ω are in kilometers, then L_0 and W_0 will also be in kilometers. The quantity K (in kilometers) can be calculated from

$$K = \frac{2.30 \times 10^5 \, T^1/m}{k^2 \cdot \sin^2 \varphi} \qquad \text{(D-29)}$$

where T^1 = thrust or tow line tension (kg), and m = iceberg mass (kg).

After computing the thrust angle with Fig. D-11, the speed is given with the aid of Fig. D-12. A numerical factor has been introduced so that the speed is obtained in knots if W_0 is in kilometers.

PROPELLER POWER REQUIREMENTS

Efficient towing at low speeds requires large, low-speed propellers. At very low speeds, the thrust of a given propulsion system approaches a constant value although the efficiency approaches zero as the speed approaches zero. Thus, at very low speed, it is convenient to describe the force per unit of available power as a function of the available power per unit area engaged by the propeller system:

$$\frac{\text{Thrust}}{\text{Power}} = f\left(\frac{\text{Power}}{\text{Area}}\right) .$$

The relation is not entirely unique and depends upon details of the propeller design (i.e., pitch, diameter, number of blades, blade thickness, blade width, etc.). The relation plotted in Fig. D-13 is based upon a three-bladed propeller with characteristics described by Rossell and Chapman [43]. The pitch/diameter ratio is chosen for maximum efficiency at each power/area ratio, but is approximately 0.6 in all cases. Other assumptions are: speed = 1 kn, wake fraction = 0.05, thrust deduction coefficient = 0.025, and power transmission losses = 0.05. The dashed region where the power/unit area exceeds about 235 is the region where cavitation can be expected for propellers with expanded area ratios of 0.5.

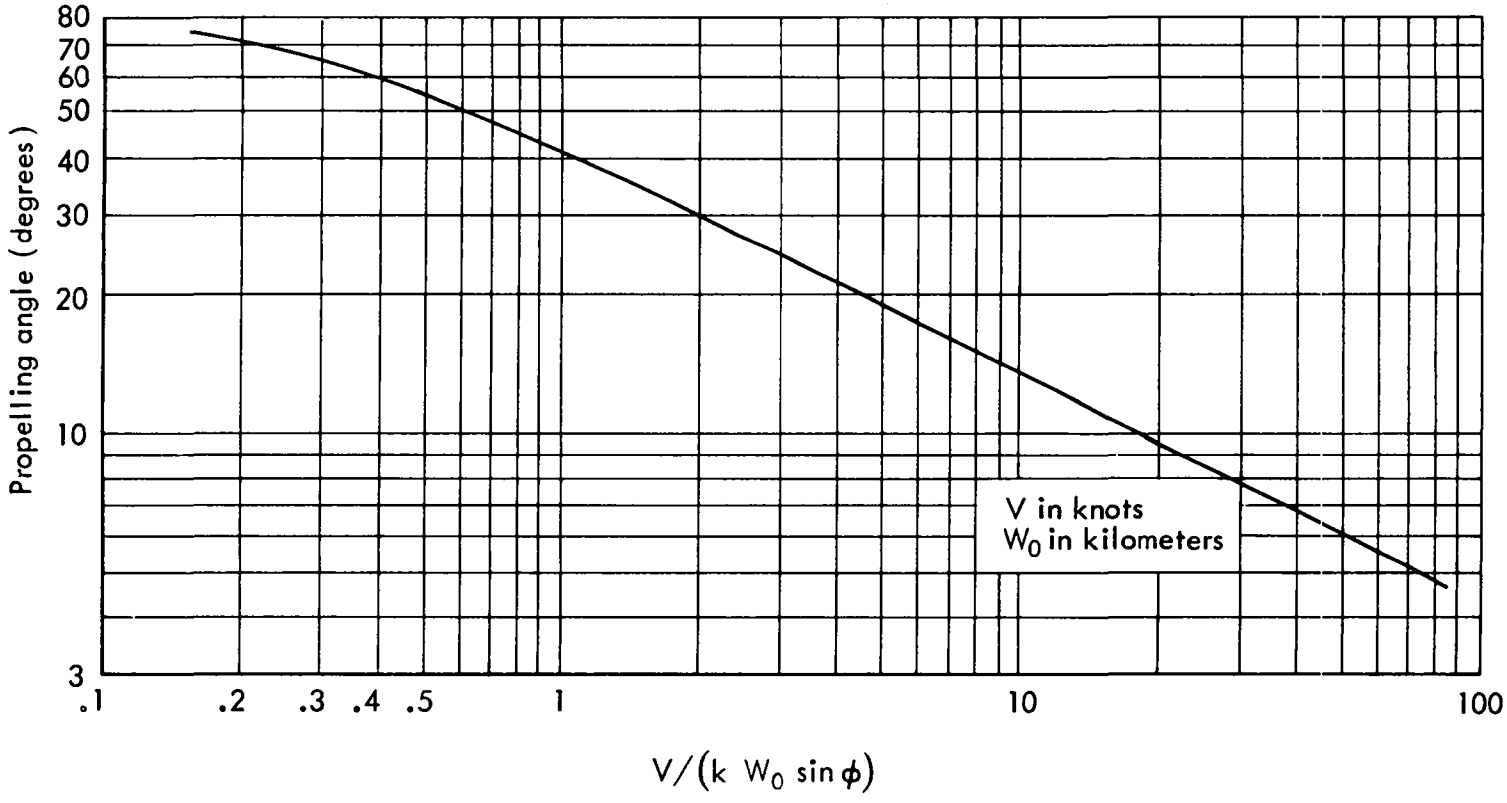

Fig. D-12 — Generalized solution for propelled speed

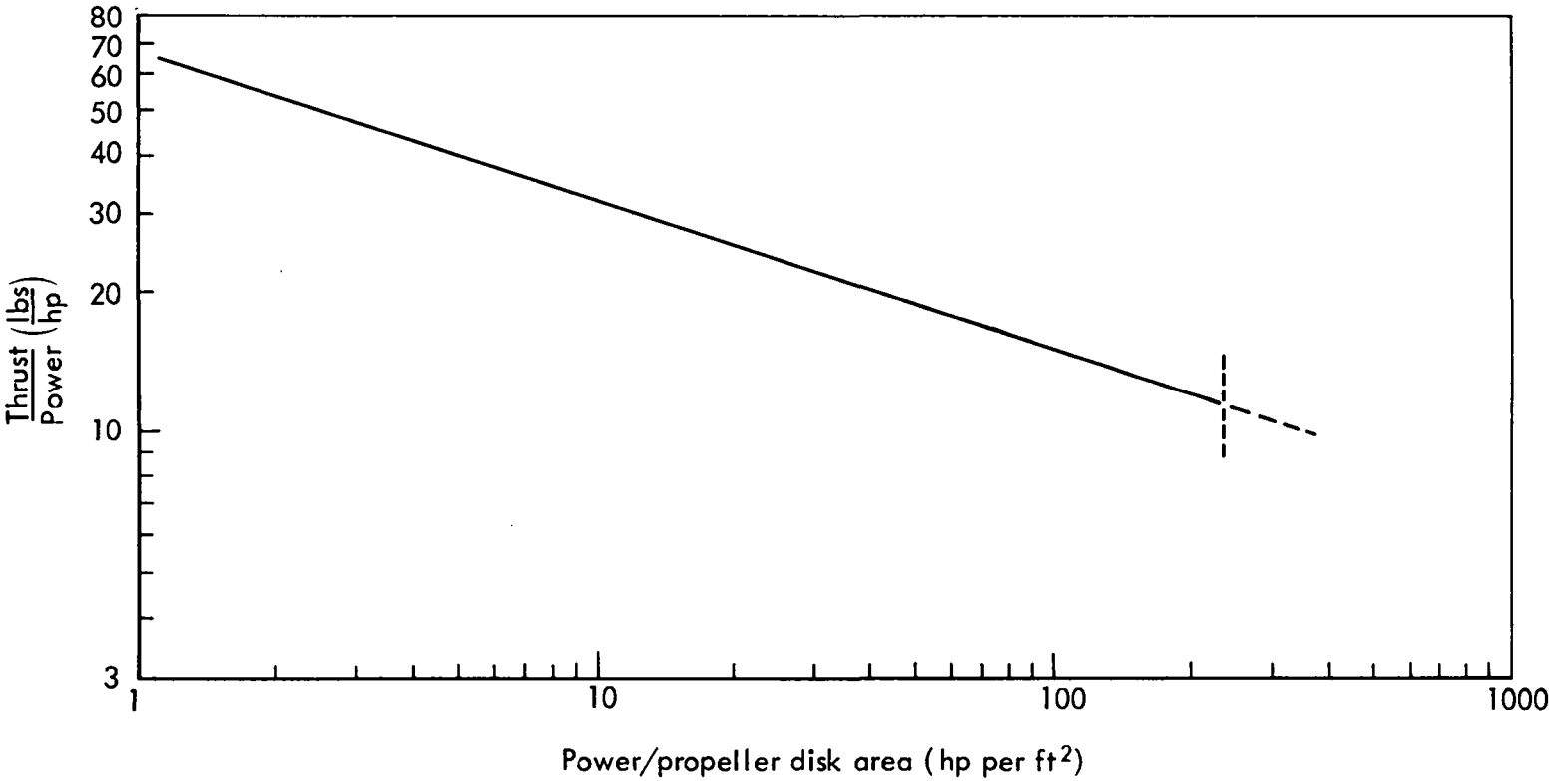

Fig. D-13 — Thrust-power-area relationship (I)

Figure D-13 is useful for deriving curves of the force that can be developed by various propeller areas under the constraint of fixed power. An alternative arrangement of the relation is given in Fig. D-14, which can be used to compute the power required versus propeller area at fixed thrust.

Figure D-15 illustrates the decline in required power as the propeller area is increased by increasing the number of propellers. This example is based upon supplying a total thrust of 10^8 N (2.2×10^7 lbs) with N propellers each 36 ft in diameter and sweeping out an area of $(\pi/4) \cdot 36^2 = 1020$ ft^2.

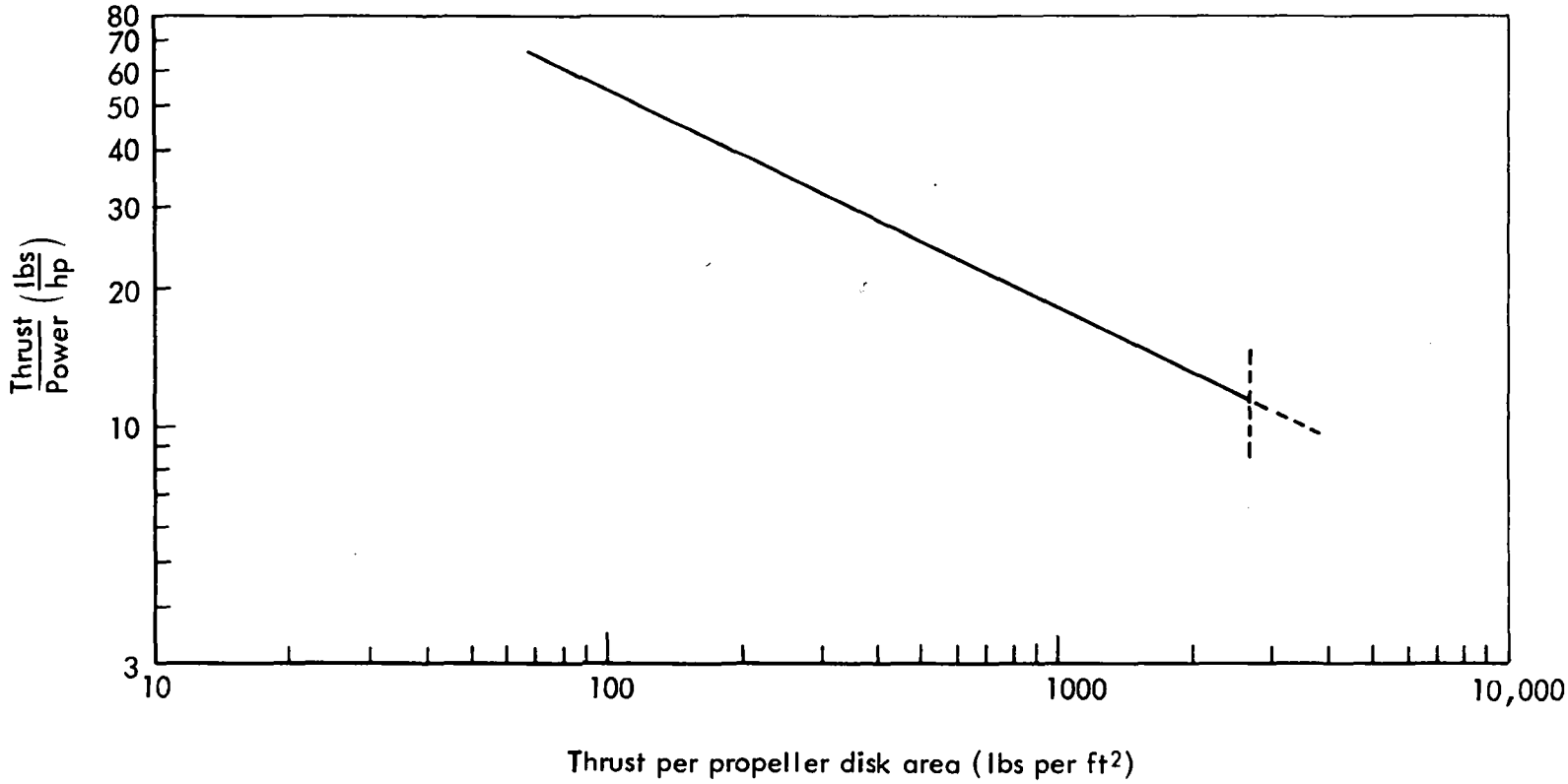

Fig. D-14 — Thrust-power-area relationship (II)

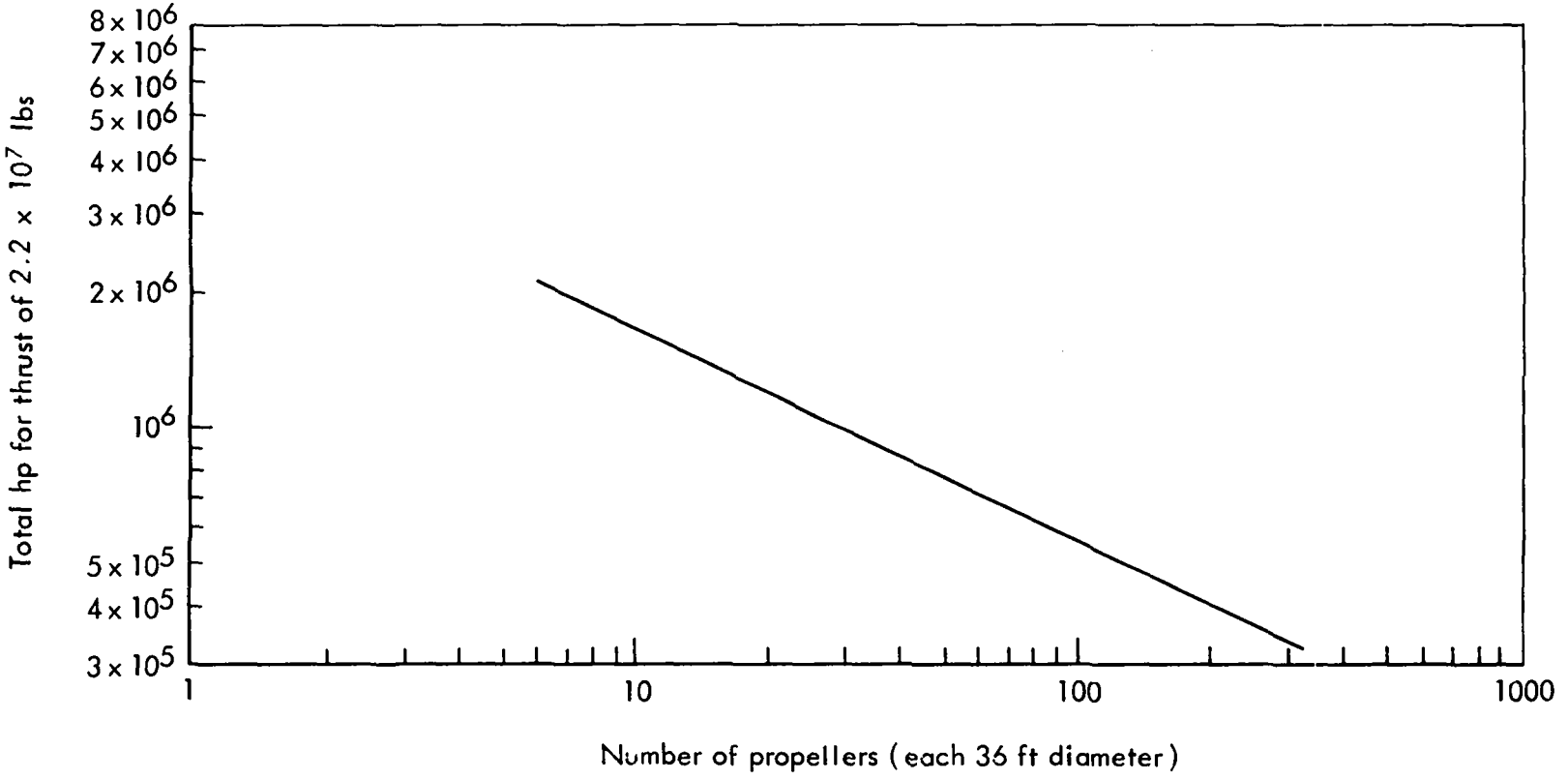

Fig. D-15 — Total power required vs number of propellers

Appendix E

THE FLOW AROUND A SUBMERGED MOVING BODY

In estimating the Coriolis coefficient k, reference has been made to the mass of rearward-flowing displaced water that attends the motion of a vessel through the water. The existence of this action can hardly be doubted; certainly no one believes that a moving ship excavates a trench by pushing before it an *ever-increasing* mass of water. Although such qualitative concepts as the familiar fact that water flows downhill suggest that the rearward-flowing displaced water is restricted to the vicinity of the ship, it would be good to have some better estimate of the scale on which this sea-surface readjustment occurs. That is, if the adjustment is over a region that is very large relative to the size of the ship, then the concept of a mass of rearward-flowing displaced water becomes vague, and an intimate exchange of momentum between the displaced water and the ship is difficult to visualize.

A second and somewhat confusing concept arises when virtual mass is identified as a mass of water moving with or being carried along by the ship motion. Note that the motion of a ship through an incompressible fluid is attended by a disturbance of the surrounding water. The water in the vicinity acquires a velocity field relative to water at rest at remote distances. Thus there is a kinetic energy field associated with the moving ship. If the ship is to accelerate, energy must be added to increase both the kinetic energy of the ship and the energy of the hydrodynamic velocity field. It is purely an arbitrary convention that this incremental energy is characterized by the ship speed and a virtual mass. When choosing the characteristic speed, it might

equally as well be -U (for a ship speed U) since only U^2 appears in defining the virtual mass. The choice of the negative sign would be more harmonious with the concept of rearward-flowing displaced fluid; at least there would not be the paradoxical situation of two different masses of fluid moving in opposite directions.

The basis of the virtual mass theory lies in the treatment of the irrotational flow of an inviscid, incompressible fluid around a submerged sphere or cylinder. The domain of the fluid is infinite; the fluid is at rest at infinity; and the object is in uniform rectilinear motion. Although some questions will undoubtedly arise over the equivalence of flow around a fully submerged object and a surface vessel, it is equally clear that submarines do not bore tunnels; rather, the water is accelerated around the submarine in the course of its progress. The approximation involved in equating the submerged flow to the surface-bounded flow is made plausible by the empirical fact that the same virtual mass results are applied to both surface ships and submarines. In practice, the surface perturbation effect is therefore apparently small; the ship moves by accelerating the water around the hull in a manner that is nearly the same as that accomplished by submarines. Since this is an empirical equivalence pertaining to well-formed hulls, one may rightfully hold some reservations about surface effects when very blunt-ended objects are in motion on the sea surface.

The correct interpretation of the virtual mass theory is not contradictory to the concept of rearward-flowing, displaced fluid. This fact can be illustrated by examining the problem of a moving submerged sphere. For that simple problem, the following relevant questions can be stated *and* resolved:

- In a physical sense, is there a mass of rearward-flowing, displaced water? If so, what measure of its spatial extent can be derived?
- In a physical sense, is there a mass of water moving with the object (the virtual mass)? If so, what measure of its physical extent can be derived?

For the irrotational flow of an inviscid, incompressible fluid, the velocity components can be derived from a potential. For a sphere moving through a fluid that is at rest at infinity, the potential in spherical polar coordinates is given by Ref. 44:

$$\phi = \tfrac{1}{2} U \left(\frac{a^3}{r^2}\right) \cos \Theta \ . \qquad \text{(E-1)}$$

The sphere of radius, a, is moving at speed U in the direction of increasing z (left to right), and Θ is a polar angle measured from the positive z axis. The sphere is shown at the instant its center crosses the xy plane. At that instant, the xy plane is also the equatorial plane of the sphere. These coordinates are illustrated in Fig. E-1. Because of the axial symmetry about the z axis, there are no azimuthal velocity components. The radial and polar coordinate components are

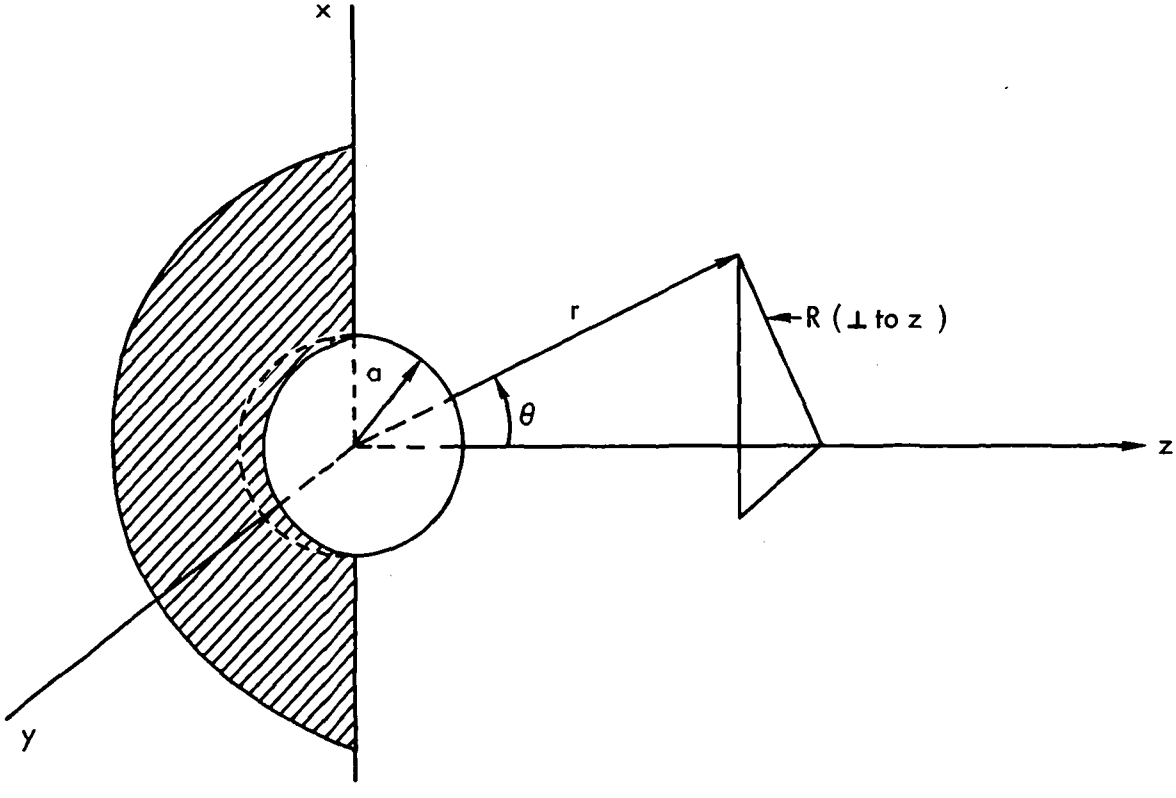

Fig. E-1 — Moving sphere and coordinate frames

$$v_r = -\frac{\partial \phi}{\partial r} = U\left(\frac{a^3}{r^3}\right)\cos\,\Theta\ . \tag{E-2}$$

$$v_\Theta = -\frac{1}{r}\frac{\partial \phi}{\partial \Theta} = \tfrac{1}{2}\,U\left(\frac{a^3}{r^3}\right)\sin\,\Theta\ . \tag{E-3}$$

The disturbance is confined to the vicinity of the sphere. The velocities at a distance of two diameters (r = 4a) are less than 2 percent of the speed at the surface of the sphere (r = a).

The velocity components are sometimes confusing in spherical polar coordinates. A discussion of these components is more convenient in terms of cylindrical coordinates R,z. The conversion to cylindrical coordinates is accomplished by:

$$v_z = v_r\,\cos\,\Theta - v_\Theta\,\sin\,\Theta\ ,$$

$$v_R = v_r\,\sin\,\Theta + v_\Theta\,\cos\,\Theta\ .$$

Applying this transformation to the velocity components, v_r and v_Θ, will yield

$$v_z = U\left(\frac{a^3}{r^3}\right)(\cos^2\,\Theta - \tfrac{1}{2}\sin^2\,\Theta)\ . \tag{E-4}$$

$$v_R = \frac{3}{2}\,U\left(\frac{a^3}{r^3}\right)\sin\,\Theta\,\cos\,\Theta\ . \tag{E-5}$$

This is an incomplete coordinate reduction. The point at which velocity components are defined is specified by r,Θ, but the velocity components are axial and radial (cylindrical) components.

The radial motions v_R vanish at $\Theta = 0$ (on the z axis), a requirement obviously arising from the axial symmetry. They also vanish at $\Theta = \pi/2$, where the entirety of the velocity is manifested by the axial component, v_z.

The axial component has a maximum value of +U at two points on the sphere r = a: $\Theta = 0$ and $\Theta = \pi$, both of which lie on the z axis and correspond to the stagnation points. The fluid velocity at these points is zero relative to the sphere velocity, but is indeed U relative to fluid at rest at infinity. The axial velocity at $\Theta = \pi/2$ (the equatorial plane of the sphere) is

$$v_z = -\frac{1}{2} U \left(\frac{a^3}{R^3} \right) .$$

In this equatorial plane (z = 0), the axial velocity is negative (leftward moving) for all radii ($a \leq R < \infty$).

The total mass flow across the plane z = 0 is readily computed by

$$= 2\pi\rho \int_{R=a}^{\infty} v_z R' \, dR = -\pi\rho U a^3 \int_a^{\infty} \frac{dR}{R^2} , = -\pi a^2 \rho U . \qquad \text{(E-6)}$$

This quantity is the negative of the rate at which volume is swept out by the advancing cross section of the sphere. In this z = 0 plane, there is no evidence of a forward moving mass of water. Instead, the velocity is always negative and can be interpreted as the rearward-flowing mass of displaced water.

According to Eq. (E-4), regions identified by $0 < \tan\Theta < 2$ and $-2 < \tan\Theta < 0$ will be characterized by positive v_z. Although it is tempting to refer to these as the regions in which fluid is being carried along by the sphere, it is also evident that these regions contain the extremes of radial velocities (positive in the leading zone, negative in the trailing zone), and hardly conform with the word picture of forward motion.

The common result of the virtual mass calculation can be easily obtained by integrating the kinetic energy density over all space. This is most easily done in the original spherical polar coordinate system with the kinetic energy density ε defined as

$$\varepsilon = \frac{1}{2}\rho \left(v_r^2 + v_\Theta^2 \right) = \frac{1}{2}\rho U^2 \frac{a^6}{r^6} \left(\cos^2\Theta + \frac{1}{4} \sin^2\Theta \right) .$$

The energy integral is

$$T' = 2\pi \int_a^\infty \int_{\Theta=0}^{\pi} \varepsilon \cdot \sin\Theta \, d\Theta \, r^2 \, dr = \frac{1}{3} \pi a^3 \rho U^2 \, . \qquad \text{(E-7)}$$

This usual result can be attributed to a virtual mass $M' = (2/3)\pi a^3 \rho$, which appears as if it had kinetic energy:

$$T' = \frac{1}{2} M' U^2 \, .$$

The appearance is not the reality, however, and there is no easily identifiable mass M' that moves at speed U. All sense of directionality is lost when forming the positive-definite energy density.

If the integration (E-7) is done first over Θ and then over a region from a to r (instead of a to ∞), it can be shown that one-half of the kinetic energy lies within a sphere of radius $\sqrt[3]{2} \cdot a$, which corresponds to a fluid shell of thickness 0.26a surrounding the sphere. Thus a substantial fraction of the disturbance is quite local rather than diffuse.

REFERENCES

1. Engel, L., and the Editors of LIFE, *The Sea,* LIFE Nature Library, TIME Inc., New York, 1961.
2. Weeks, W. F., and W. J. Campbell, *Icebergs as a Fresh Water Source: An Appraisal,* presented at the Symposium on Hydrology of Glaciers, Cambridge, England, September 1969.
3. Weeks, W. F., and W. J. Campbell, *Icebergs as a Fresh Water Source: An Appraisal,* Research Report 200, Cold Regions Research and Engineering Laboratory, Hanover, New Hampshire, January 1973.
4. Bowditch, N., *American Practical Navigator,* H.O. Pub. No. 9, U.S. Government Printing Office, Washington, D.C.
5. Dyson, James L., *The World of Ice,* Alfred A. Knopf, New York, 1956.
6. Armstrong, Ellis L. (Commissioner, Bureau of Reclamation), *New Technology for Water Resource Development,* an address before the American Society of Civil Engineers at the National Water Resources Engineering Conference, Phoenix, Arizona, January 12, 1971.
7. Holý, Miloš, *Water and the Environment,* Food and Agriculture Organization of the United Nations, Rome, 1971.
8. Moss, Frank E., *The Water Crisis,* Frederick A. Praeger, New York, 1967.
9. Murray, C. R., *Estimated Use of Water in the United States-1965,* Geological Survey Circular No. 556, Washington, D.C., 1968.
10. Piper, A. M., *Has the United States Enough Water?* Geological Survey Water Supply Paper 1797, U.S. Government Printing Office Cat. No. I, 19.13:1797, Washington, D.C., 1965.
11. Popkin, R., *Desalinization: Water for the World's Future,* Frederick A. Praeger, New York, 1968.
12. Thomas, Harold E., "Water Laws and Concepts," *EOS* (Transactions, American Geophysical Union), Vol. 50, 1969, pp. 40-50.
13. *Alternatives in Water Management,* National Academy of Sciences, National Research Council, Publication No. 1408, Washington, D.C., 1966.
14. *Better Water for Americans,* American Water Works Association, New York, 1967.
15. *The Nation's Water Resources,* Water Resources Council, U.S. Government Printing Office, Washington, D.C., 1968.

16. *Water Resources Use and Management,* Proceedings of a Symposium held at Canberra by the Australian Academy of Science, 9-13 September 1963, Melbourne University Press, 1964.
17. *Water Supply and Sewerage,* Sector Working Paper, World Bank, Washington, D.C., October 1971.
18. Howe, Charles W., and K. William Easter, *Interbasin Transfers of Water,* Resources for the Future, Inc., The Johns Hopkins Press, Baltimore, Maryland, 1971.
19. Wollman, Nathaniel, *The Water Resources of Chile,* Resources for the Future, Inc., The Johns Hopkins Press, Baltimore, Maryland, 1968.
20. Singer, S. Fred, "Human Energy Production as a Process in the Biosphere," *Scientific American,* Vol. 223, No. 3, pp. 174-176, September 1970.
21. Penman, H. L., "The Water Cycle," *Scientific American,* Vol. 223, No. 3, pp. 98-100, September 1970.
22. *Atlas Antarktiki* (Atlas of Antarctica), published in 1966 in Moscow by the Main Administration of Geodesy and Cartography, Ministry of Geology USSR, in accordance with a resolution of the Presidium of the Academy of Sciences USSR. Translated in *Soviet Geography: Review and Translation,* Vol. VIII, Nos. 5-6, May-June 1967, Lane Press, Burlington, Vermont.
23. Bently, C. R., "The Structure of Antarctica and Its Ice Cover," in Hugh Odishaw, ed., *Research in Geophysics,* Vol. 2, MIT Press, Massachusetts Institute of Technology, Cambridge, Massachusetts, 1964.
24. Swithinbank, C., "The Ice Shelves," in T. Hatherton, ed., *Antarctica,* Methuen and Co., Ltd., London, 1965.
25. Hatherton, Trevor, ed., *Antarctica,* Frederick A. Praeger, New York, 1965.
26. Gordienko, P. A., "The Role of Icebergs in the Ice and Thermal Balance of Coastal Antarctic Waters (translation)," *Problemy Arktiki i Antarktiki,* Vol. 2, 1960, pp. 17-22.
27. Gow, Anthony J., *Electrical Conductivity of Snow and Glacier Ice from Antarctica and Greenland,* Cold Regions Research and Engineering Laboratory, Research Report 248, Hanover, New Hampshire, October1968.
28. Rossell, Henry E., and Lawrence B. Chapman, *Principles of Naval Architecture,* The Society of Naval Architects and Marine Engineers, New York, 1958.
29. Hoerner, S. F., *Fluid-Dynamic Drag,* Hoerner, Midland Park, New Jersey, 1965.
30. *Lower Colorado Region, Comprehensive Framework Study of Water and Land Resources, Main Report June 1971,* prepared by Lower Colorado Region State-Federal Interagency Group for the Pacific Southwest Interagency Committee Water Resources Council, Boulder City, Nevada.
31. Milne-Thomson, L. M., *Theoretical Hydrodynamics,* 2d ed., The Macmillan Company, New York, 1950, p. 413.
32. Kays, W. M., *Convective Heat and Mass Transfer,* McGraw-Hill Book Company, New York, 1966.
33. Bowers, H. L., et al., *Estimated Capital Costs of Nuclear and Fossil Power Plants,* Oak Ridge National Laboratory, Oak Ridge, Tennessee, March 5, 1971.
34. Culler, Floyd L., and William O. Harms, "Energy from Breeder Reactors," *Physics Today,* Vol. 25, No. 5, May 1972, pp. 28-39.

35. *Peaceful Uses of Atomic Energy,* Vol. 2, *Performance of Nuclear Plants, Costing of Nuclear Plants, Fuel Management,* United Nations and the International Atomic Energy Agency, Vienna, 1972.
36. Hubbard, Michael, "The Comparative Costs of Oil Transport to and Within Europe," *Journal of the Institute of Petroleum,* Vol. 53, No. 517, January 1967, pp. 1-23.
37. Johnson, R. P., and H. P. Rumble, *Determination of Weight, Volume, and Cost for Tankers and Dry Cargo Ships,* The Rand Corporation, RM-3318-1-PR, April 1968.
38. Sudbury, John D., "New Concept Proposes Towing Submerged Barges at Controlled Depth," *Canadian Petroleum,* August 1972, pp. 18-23.
39. *Atlas of Pilot Charts, South Pacific and Indian Oceans,* H.O. Pub. No. 107, U.S. Naval Oceanographic Office, Washington, D.C., 1969.
40. *Atlas of Surface Currents Northeastern Pacific Ocean,* H.O. Pub. No. 570, U.S. Navy, Washington, D.C., 1967.
41. *Pilot Chart of the North Pacific Ocean,* N.O. 55, U.S. Naval Oceanographic Office, Washington, D.C., 1972.
42. *Quarterly Surface Current Charts of the South Pacific Ocean,* Met. 0. 435, Her Majesty's Stationery Office, London, 1967.
43. Rossell, H. C., and L. B. Chapman, *Principles of Naval Architecture,* Vol. 2, The Society of Naval Architects and Marine Engineers, New York, 1958, p. 164.
44. Lamb, Horace, *Hydrodynamics,* Dover Publications, New York, 1945, p. 123.

SELECTED BIBLIOGRAPHY

Annual Report of Progress on Engineering Research, U.S. Department of Interior, Bureau of Reclamation, U.S. Government Printing Office, Washington, D.C.

Bibliography on Social-Economic Aspects of Water Resources, 1966, U.S. Government Printing Office Cat. No. I, 1.89:W29, Washington, D.C.

The California State Water Project in 1971, Department of Water Resources Bulletin No. 132-71, Sacramento, California, June 1971.

Catalog of Water Resources Research, compiled by the Science Information Exchange of the Smithsonian Institute, Vol. I (Parts 1 and 2, 1965), Vol. II (1966), U.S. Government Printing Office, Washington, D.C.

Data Users Handbook, NASA Earth Resources Technology Satellite, Goddard Space Flight Center, Greenbelt, Maryland.

DeHaven, J. C., L. A. Gore, and J. Hirshleifer, *A Brief Survey of the Technology and Economics of Water Supply,* The Rand Corporation, R-258-RC, October 1953.

Eckert, E.R.G., and R. M. Drake, *Heat and Mass Transfer,* McGraw-Hill Book Company, New York, 1959.

First Annual Report 1970-1971, Arizona Water Commission, Phoenix, Arizona, 1971.

Fletcher, J. O., *Ice Extent in the Southern Ocean and Its Relation to World Climate,* The Rand Corporation, RM-5793-NSF, March 1969.

Gow, Anthony J., *The Inner Structure of the Ross Ice Shelf at Little America V, Antarctica, as revealed by Deep Core Drilling,* International Union of Geodesy and Geophysics (Commission of Snow and Ice, Berkeley,) Publication 61, 1963.

Hill, N. N., ed., *The Sea,* Interscience Publishers, New York, 1966.

Hirshleifer, J., J. C. DeHaven, and J. Milliman, *Water Supply: Economics, Technology, and Policy,* University of Chicago Press, Chicago, Illinois, 1969.

Hoehn, W. E., *The Economics of Nuclear Reactors for Power and Desalting,* The Rand Corporation, RM-5227-1-PR/ISA, November 1967.

Hoehn, W. E., *Prospects for Desalted Water Costs,* The Rand Corporation, RM-5971-FF, October 1969.

Howe, Charles W., et al., *Inland Waterway Transportation Studies in Public and Private Management and Investment Decisions,* Resources for the Future, Inc., The Johns Hopkins Press, Baltimore, Maryland, 1969.

Hughes, T., *Ice Streamline Cooperative Antarctic Project,* ISCAP Bulletin No. 1, Institute of Polar Studies, Ohio State University, Columbus, Ohio, June 1972.

Huschke, R. E., R. R. Rapp, and C. Schutz, *Meteorological Aspects of Middle East Water Supply,* The Rand Corporation, RM-6267-FF, March 1970.

Kollmeyer, R. C., *Interim Report on Iceberg Deterioration,* U.S. Coast Guard Oceanographic Report No. 11, Washington, D.C., 1966.

Magin, G. B., and L. E. Randall, *Review of Literature on Evaporation Suppression,* Geological Survey Professional Paper 272-C, Washington, D.C., pp. 53-69.

Martin, L., "James Eights' Pioneer Observations and Interpretation of Erratics in Antarctic Icebergs," *Geological Society of America. Bulletin* Vol. 60, January 1949, pp. 177-181.

McGinnies, W. G., and B. J. Goldman, eds., *Arid Lands in Perspective,* University of Arizona Press, Tucson, Arizona, 1969.

McGuiness, C. L., *Role of Ground Water in the National Water Situation (1963),* U.S. Government Printing Office Cat. No. I, 19.13:1800, Washington, D.C.

McKean, R. N., *Efficiency in Government through Systems Analysis: With Emphasis on Water Resource Development,* John Wiley & Sons, Inc., New York, 1959.

Meinzer, O. E., *The Occurrence of Ground Water in the United States with a Discussion of Principles,* Water Supply Paper, Geological Survey (1923, 1959 printing), U.S. Government Printing Office Cat. No. I, 19.13:489, Washington, D.C.

Neuman, G., *Ocean Currents,* Elsevier Publishing Co., New York, 1968.

North American Water and Power Alliance, NAWAPA, Ralph M. Parsons Co., Los Angeles, 1965.

Physical Characteristics of the Antarctic Ice Sheet, American Geographical Society, Folio 2, Antarctic Map Folio Series, New York, 1964.

Polar Research, A Survey, National Academy of Sciences, Washington, D.C., 1970.

Potter, Neal, *Natural Resource Potentials of the Antarctic,* American Geographical Society Occasional Publication No. 4, 1969, The Lane Press, Burlington, Vermont.

Project Skywater 1969 Annual Report, U.S. Department of Interior, Bureau of Reclamation, Office of Atmospheric Water Resources, Report No. REC-OCE-70-13, Denver, Colorado.

Publications of the Geological Survey, Geological Survey (1967 with periodic supplements), Washington, D.C.

Quann, Louis O., ed., *Research in the Antarctic,* AAAS Publication No. 93, Washington, D.C., 1971.

Reconnaissance Report, Augmentation of the Colorado River by Desalting of Sea Water, Bureau of Reclamation, Department of Interior, Washington, D.C., 1968.

Saline Water Conversion Engineering Data Book (1965), U.S. Government Printing Office Cat. No. I, 1.77/2, Sa3, Washington, D.C.

Saline Water Conversion Report, Annual Report, 1969-70, U.S. Department of Interior, Office of Saline Water, U.S. Government Printing Office, Washington, D.C.

Scholander, P. F., J. W. Kanwisher, and D. C. Nutt, "Gases in Icebergs," *Science,* Vol. 123, January 20, 1956, pp. 104-105.

Scholander, P. F., and D. C. Nutt, "Bubble Pressure of Greenland Icebergs," *Journal of Glaciology* (London), Vol. 3, October 1960, pp. 671-678.

Shil'nikov, V. I., "Volume and Number of Icebergs in the Antarctic (from 44° to 168°E)," *Soviet Antarctic Expedition Information Bulletin,* Vol. 3, 1965, pp. 23-26.

Shumskiy, P. A., A. N. Krenke, and I. A. Zofikov, "Ice and Its Changes," in Hugh Odishaw, ed., *Research in Geophysics,* Vol. 2, MIT Press, Massachusetts Institute of Technology, Cambridge, Massachusetts, 1964.

Thirty-Third Annual Report 1971, The Metropolitan Water District of Southern California, Los Angeles, California, 1971.

Thomas, R. H., and P. H. Coslett, "Bottom Melting of Ice Shelves and the Mass Balance of Antarctica," *Nature,* Vol. 228, October 3, 1970, pp. 47-49.

Todd, David Keith, ed., *The Water Encyclopedia,* Water Information Center, Port Washington, New York, 1970.

Ueda, Herbert T., and Donald E. Garfield, *Deep Core Drilling at Byrd Station, Antarctica,* ISAGE Symposium, Hanover, New Hampshire, 3-7 September 1968.

Ward, Barbara, and René Dubos, *Only One Earth,* W. W. Norton & Company, Inc., New York, 1972.

Water Resources Research Catalog, U.S. Department of Interior, Office of Water Resources Research, U.S. Government Printing Office, Washington, D.C.

Wooster, W. S., "Eastern Boundary Currents in the South Pacific," in W. S. Wooster, ed., *Scientific Exploration of the South Pacific,* Printing and Publishing Office, National Academy of Sciences, Washington, D.C., 1970.

World Atlas of Sea Surface Temperatures, H.O. Pub. No. 225, U.S. Navy, Washington, D.C., 1969.

Yen, Yin-Chao, *Analytical and Experimental Study of a Melting Problem with Natural Convection,* Cold Regions Research and Engineering Laboratory, Research Report 234, Hanover, New Hampshire, July 1967.